

AD 622563

FORM 1-60
AUGUST 1965
INSTRUMENTATION PAPERS, NO. 25



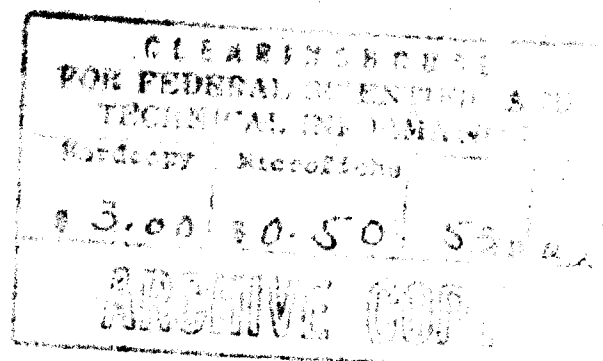
AIR FORCE CAMBRIDGE RESEARCH LABORATORIES

1. G. HANSCOM FIELD, BEDFORD, MASSACHUSETTS

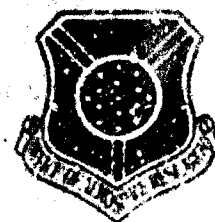
A Ray-Tracing Program for Birefringent Filters

J. M. BECKERS

R. B. DUNN



OFFICE OF AEROSPACE RESEARCH
United States Air Force



AFCRL-65-605
AUGUST 1965
INSTRUMENTATION PAPERS, NO. 75

SPACE PHYSICS LABORATORY PROJECT 7649

AIR FORCE CAMBRIDGE RESEARCH LABORATORIES

L. G. HANSCOM FIELD, BEDFORD, MASSACHUSETTS

A Ray-Tracing Program for Birefringent Filters

**J. M. BECKERS
R. B. DUNN**

**OFFICE OF AEROSPACE RESEARCH
United States Air Force**



Abstract

A computer program for determining the transmission of birefringent filters is described. This program is used for the following investigations:

- (a) The feasibility of the construction of a birefringent filter that will work simultaneously for wavelengths of 3933.3, 6562.8, and 10830.3 Ångstroms. These three wavelengths are of particular importance for solar studies.
- (b) The off-axis characteristics of Solc filters.
- (c) The tolerances required for the elements of a Solc filter.
- (d) The influence of imperfect polarizers on the transmission characteristics of Lyot filters.

Contents

1. INTRODUCTION	1
2. DESCRIPTION OF THE COMPUTATION PROGRAM	2
2.1 On-Axis Rays	2
2.2 Off-Axis Rays	4
2.3 Imperfect Polarizers	9
3. APPLICATIONS	9
3.1 Introduction	9
3.2 A Birefringent Filter for the Solar K, H $_{\alpha}$, and He-10830 Lines	10
3.3 Off-Axis Characteristics of Solc Filters	24
3.4 Lyot Filters with Imperfect Polarizers	31
3.5 Tolerances for Solc Filters	34
4. CONCLUSIONS	37
ACKNOWLEDGMENTS	41
REFERENCES	41

Illustrations

1. Definition of α and ϕ	8
2. Layout of the Three-Line Filter	15
3. On-Axis Transmission of Three-Line Filter at K (3933.3 Å)	17
4. On-Axis Transmission of Three-Line Filter at H $_{\alpha}$ (6562.8 Å)	18

Illustrations

5.	Integrated Parasitic Transmissions T_p for Various Wavelength Intervals Centered on the Principal Wavelengths Expressed in the Transmission of the Main Band T_m	19
6.	Integrated Parasitic Intensities I_p for Various Wavelength Intervals Centered on the Principal Wavelengths Expressed in the Intensity of the Main Band I_m	20
7.	On-Axis Transmission of Three-Line Filter at He-10830	23
8.	On-Axis Transmission of Two Types of Solc Filters as Compared with a Comparable Lyot Filter	27
9.	Off-Axis Transmission Profile of a Solc-D Filter and of a Solc-CC Filter	30
10.	The Effect of Imperfect Polarizers on 4-Element On-Axis Lyot Filter Transmission	33
11.	Ratio T_p/T_m for a Solc-C Filter with Various Tolerances for the Plate Thicknesses and Orientations	36
12.	Ratio T_p/T_m for an 18-Plate Solc-C Filter for which Only One Plate Has a 0.05-Order Imperfection as a Function of the Plate Position	38
13.	Ratio T_p/T_m for Solc-A Filters	39

Tables

1.	Ray-Tracing Program in Fortran IID	5
2.	Composition of the Filter for the K, H_α , and He-10830 Line	13
3.	Orientations of the $\lambda/2$ Plates for the K-Line Filter	16
4.	Relative Amount of Parasitic Transmissions for Bands of Various Widths Centered on the K-Line	16
5.	Orientation of $\lambda/2$ Plates for the H_α Filter	21
6.	Relative Amount of Parasitic Transmissions for Band of Various Widths Centered on the H_α Line	21
7.	Orientation of $\lambda/2$ Plates for the He-10830 Line	22
8.	Relative Amount of Parasitic Transmission for Bands of Various Widths Centered on the He-10830 Line	22
9.	Composition of the Solc-A Filter	25
10.	Composition of the Solc-B Filter	25
11.	Composition of the Solc-C Filter	26

Tables

12. Composition of the Solc-D Filter	28
13. Shift of Transmission Band for Off-Axis Rays for Five Types of Solc Filters	29
14. Composition of the Solc-CC Filter	31
15. Influence of Errors in Plate Orientation and Thickness on T_p/T_m	35

A Ray-Tracing Program for Birefringent Filters

I. INTRODUCTION

Birefringent filters utilize the variation of the retardation of birefringent plates with wavelength to isolate certain regions in the optical wavelength spectrum. This variation is due mainly to the variation of the plate thickness expressed in wavelengths. In the most frequently used materials, quartz and calcite, it is counteracted by an increase of the birefringence with wavelength.

The above-mentioned principle to isolate certain wavelengths was probably first applied by Mascart (1874) when he used it to separate the sodium D_1 and D_2 lines. Today, the best known applications are the Lyot-Öhman type filter (Lyot, 1944; Evans, 1949) and the Šolc type filter (Šolc, 1959; Šolc, 1960; Šolc, 1965; Evans, 1958). The Lyot filter, in its basic form, consists of a chain of independent segments each composed of a birefringent plate placed between either crossed or parallel polarizers having angles of 45 deg with the plate's retardation axis. One such segment produces periodic intensity patterns in the spectrum of the transmitted light, the so-called channel spectrum. The thickness of successive segments differs by factors of two in the Lyot Filter, thereby suppressing the entire spectrum except for those regions where all the segments have simultaneous transmission maxima. One of the disadvantages of this filter is its low transmission due to the great number of polarizers used. Evans (1949) introduced a modification of the Lyot-Öhman

(Received for publication 21 June 1965)

filter that eliminated about half of the polarizers, thereby substantially improving the transmission. The Solc filter on the other hand needs only the minimum number of polarizers — two. It consists of a chain of identical retardation plates with varying position angles placed between two polarizers.

In the case of the simplest Lyot-Öhman and Solc filters, it has been possible to give analytical expressions for the filter transmission for on-axis rays [see, for example, Lyot (1944) and Evans (1958)]. For any possible arrangements of retardation plates and polarizers the computation of the transmission in the form of analytical expressions becomes very difficult. Therefore, it seemed desirable to write a computer program to determine the transmission of any chain of retardation plates and polarizers for on-axis and off-axis rays. This paper describes such a program. The utilization of imperfect polarizers is also included, since Giovanelli and Jefferies (1954) predict that the use of imperfectly polarizing polarizers may improve the transmission characteristics of Lyot filters. Section 2 describes the details of this ray-tracing program, and Section 3 describes some of its applications.

2. DESCRIPTION OF THE COMPUTATION PROGRAM

2.1 On-Axis Rays

Jones' calculus (Jones, 1941; Shurcliff, 1952) was used in the computation of on-axis rays. In this calculus each retardation plate or polarizer is mathematically represented by a set of two matrices, $S(\beta)$ and N , both having two rows and two columns. The change in polarization made by one such element on a light wave of the complex form

$$E_x = A_x \exp [i(\epsilon_x + 2\pi\nu t)] \quad \text{and} \quad E_y = A_y \exp [i(\epsilon_y + 2\pi\nu t)] \quad (1)$$

is given by

$$S(\beta) N S(-\beta) \begin{pmatrix} E_x \\ E_y \end{pmatrix}, \quad (2)$$

where β is the angle between the element axis (polarization or retardation axis) and an arbitrary x axis.

The expression for S is:

$$S(\beta) = \begin{pmatrix} \cos \beta & -\sin \beta \\ \sin \beta & \cos \beta \end{pmatrix}. \quad (3)$$

The expression for N for polarizers is:

$$N = \begin{pmatrix} p_1 & 0 \\ 0 & p_2 \end{pmatrix}, \quad (4)$$

where p_1 is the transmission along the polarizer axis and p_2 is the transmission at right angles to p_1 with $p_1 > p_2$.

For a retardation plate, the expression for N may be written as:

$$N = \begin{pmatrix} e^{i\gamma} & 0 \\ 0 & e^{-i\gamma} \end{pmatrix}, \quad (5)$$

with γ being a quantity dependent on the plate retardation (for on-axis rays) in the following manner:

$$\gamma = \pi d(\epsilon - \omega)/\lambda, \quad (6)$$

where d is the plate thickness, and ϵ and ω , as usual, the refractive indexes for the extraordinary and ordinary rays, respectively.

For a chain of polarizers or retarders, Eq. (2) is modified to

$$S(\beta_n) N_n S(-\beta_n) S(\beta_{n-1}) N_{n-1} \dots S(-\beta_2) S(+\beta_1) N_1 S(-\beta) \begin{pmatrix} E_x \\ E_y \end{pmatrix} \equiv M \begin{pmatrix} E_x \\ E_y \end{pmatrix} \quad (7)$$

which, according to Jones, can be further simplified by the relation

$$S(-\beta_i) S(\beta_{i-1}) = S(\beta_{i-1} - \beta_i). \quad (8)$$

The matrix M is found by evaluation of the matrix product in Eq. (7). The result will be a 2 by 2 matrix with complex elements. For ideal unpolarized incident light the filter transmission of the chain can be shown to be equal to the sum of the products of these matrix elements with their complex conjugates.

The computation of M is very much simplified and speeded up in the case where the filter starts with an ideal polarizer ($p_2 = 0$). Taking the x -axis to coincide with the axis of this polarizer ($\beta_1 = 0$), the first two elements of the matrix multiplication, Eq. (7), reduce to

$$\begin{pmatrix} p_1 & 0 \\ 0 & 0 \end{pmatrix}. \quad (9)$$

The last column of every subsequent multiplication will consist of zeros, and can be omitted in the multiplication.

The program is written in FORTRAN II-D language for an IBM 1620-II computer according to the calculus explained above. It is listed in Table 1. Essentially, it consists of the evaluation and multiplication of the S and N matrices, and the determination of the filter transmission from the product M. Each of the elements of the filter is specified by a punch card specifying the type of element (polarizer, quartz or calcite retardation plate); the orientation of the element's axis with respect to an arbitrary x-axis; p_2 , the imperfection of the polarizers (from now on p_1 is taken equal to 1); and, in case of retardation plates, their thickness (mm).

The coefficient of birefringence that is used to compute γ is determined by the following expressions.

For quartz the expression is written as:

$$\begin{aligned}
 (\epsilon - \omega) = & 3.8541 \times 10^{-3} + 1.07057 \times 10^{-4} / \lambda^2 + 1.9893 \times 10^{-6} / \lambda^4 \\
 & - 1.7175 \times 10^{-4} \times \lambda^2 - t \times 10^{-6} \times (1 + t/900) \\
 & \times (1.01 + 0.2 \times \lambda^2) ,
 \end{aligned} \tag{10}$$

and for calcite the expression is written as:

$$\begin{aligned}
 (\epsilon - \omega) = & -0.163724 - 3.15 \times 10^{-3} / \lambda^2 - 5.896 \times 10^{-5} / \lambda^4 \\
 & - 2.911 \times 10^{-6} / \lambda^6 + 3.037 \times 10^{-3} \times \lambda^2 + 2.54 \\
 & \times 10^{-4} \times \lambda^4 - 2.52 \times 10^{-5} \times \lambda^5 - 10^{-5} \\
 & \times [t(1.044 - 0.16\lambda) + 0.00043 t^2] ,
 \end{aligned} \tag{11}$$

where λ is expressed in microns and t is degrees centigrade.

Equation (10) was taken from a paper by M. J. Macé de Lépinay (1892); Eq. (11) was derived from the data for calcite given in the International Critical Tables. The expression for calcite is only valid for wavelengths (λ) between 3500 and 15,000 Å and temperatures (t) in the vicinity of 40°C. It fits the data to within 0.01 percent.

2.2 Off-Axis Rays

In case of off-axis rays the retardation of the quartz or calcite changes with an amount depending on the angle of incidence (φ) and the azimuth of the incident ray (α). (The incident ray α is measured from the direction of the optical axis of the

Table 1. Ray-Tracing Program in Fortran IID

```

C      TRANSMISSION PROFILE OF A BIREFRINGENT FILTER
C      MAXIMUM NUMBER OF ELEMENTS IS 50
C      S.S.1 ON=PRINTS OUT THE FILTER CONFIGURATION
C      S.S.2 ON=AT END GOES TO NEW FILTER
C      S.S.2 OFF=AT END GOES TO NEW WAVELENGTH RANGE AND ANGLE OF INCIDENCE

      DIMENSION A(50,3),X(2,4),Y(2,4),S(8)
      DIMENSION B(2),C(2)

C      FORMAT STATEMENTS

100    FORMAT(13,F4.1)
101    FORMAT(F1.0,F6.2,F9.5)
102    FORMAT(2F8.6,I4,2F6.2)
103    FORMAT(8H,LAMBDA1=F10.7,9H LAMBDA2=F10.7,12H NO. POINTS=15,7H OMEGA
1      1=F7.2,5H PHI=F7.2//)
104    FORMAT(65H,TYPE WAVELENGTH INTERVAL(MICRON) AND NUMBER OF POINTS IN
1      1 2F8.6,I4)
105    FORMAT(33H AND OMEGA AND PHI(DEG.) IN 2F6.2)
200    FORMAT(14,2X,8(E9.2))
202    FORMAT(14H,TEMPERATURE = F5.1,10H DEG.CENT.//)
203    FORMAT(64H,ELEMENT          MATERIAL          ORIENTATION          THICKNESS
1      1  CROSS)
204    FORMAT(71H
1      1  TRANSMISSION//)
205    FORMAT(32H,POLARIZER
1      1  F10.8)
206    FORMAT(32H,RET.PLATE          QUARTZ          F7.2,8H          F10.6)
207    FORMAT(32H,RET.PLATE          CALCITE          F7.2,8H          F10.6)
300    FORMAT(1X)

C      DEFINITION OF PARAMETERS

43     READ 100,N,T
      READ 101,((A(I,J),J=1,3),I=1,N)
      IF(SENSE SWITCH 1)30,31
30     PUNCH 202,T
      PUNCH 203
      PUNCH 204
      DO 32 I=1,N
        IF(A(I,1)-1.5)33,33,34
33     PUNCH 205,A(I,2),A(I,3)
        GO TO 32
34     IF(A(I,1)-2.5)35,35,36
35     PUNCH 206,A(I,2),A(I,3)
        GO TO 32
36     PUNCH 207,A(I,2),A(I,3)
32     CONTINUE
      PUNCH 300
      PUNCH 300
31     D=.017453293
      E=A(1,2)
      DO 20 J=1,N
20     A(J,2)=A(J,2)-E
      DO 70 J=2,N

```

Table 1. (Continued)

```

IF(A(J,1)-1.5)71,71,70
71 A(J,3)=SORTF(A(J,3))
70 CONTINUE
42 PRINT 104
PRINT 105
ACCEPT 102,W1,W2,M,OMEGA,PHI
PUNCH 300
PUNCH 103,W1,W2,M,OMEGA,PHI
OMEGA=(OMEGA-E)*D
PHI=PHI*D
DO 666 I=1,8
666 S(I)=0.0
KL=1
LL=1
FM=M
W2=(W2-W1)/(FM-1.)

C TRANSMISSION COMPUTATIONS

DO 1 J=1,M
KK=1
FJ=J-1
W=W1+FJ*W2
P=W*W
Q=P*P
R=P*Q
B(1)=BRFROB(W,P,Q,R,T)
B(2)=BRFCB(W,P,Q,R,T)
C(1)=FNOOB(W,T)
C(2)=FNOCB(W,T)
65 DO 2 K=1,M
IF(K-1)21,21,22
21 OM=0
CALL MATRXB(OM,Y)
Y(2,3)=0
GO TO 13
22 IF(A(K,1)-1.5)5,5,6
6 KA=A(K,1)-1.
IF(PHI)7,7,8
7 BB=B(KA)
GO TO 9
8 OM=OMEGA-A(K,2)*D
ZZ=SINF(PHI)
Z=COSF(OM)**2
BB=B(KA)*(1.-(ZZ*ZZ*((Z/C(KA))-((1.-Z)/(C(KA)+B(KA)))))/(2.*C(KA))
1)
9 G=-3.1415927*A(K,3)*(1.E+3)*BB/W
X(1,1)=COSF(G)
X(1,2)=SINF(G)
X(2,3)=X(1,1)
X(2,4)=-X(1,2)
GO TO 11
5 X(1,1)=1.
X(1,2)=0.0
X(2,3)=A(K,3)
X(2,4)=0.0

```

Table 1. (Continued)

```

11  X(1,3)=.0
    X(1,4)=.0
    X(2,1)=.0
    X(2,2)=.0
    CALL MATMPB(X,Y)
    IF(K-N)13,14,14
13  OM=(A(K,2)-A(K+1,2))*D
    GO TO 15
14  OM=A(K,2)*D
15  CALL MATRXB(OM,X)
2   CALL MATMPB(X,Y)
    TR=.0
    DO 12 L=1,2
    DO 12 MM=1,2
12  TR=TR+Y(L,MM)**2
    IF(A(1,3))60,60,61
61  GO TO (62,63),KK
62  S(LL)=TR
    DO 64 KB=2,N
64  A(KB,2)=A(KB,2)-90.
    KK=2
    GO TO 65
63  S(LL)=A(1,3)*TR+S(LL)
    DO 66 KB=2,N
66  A(KB,2)=A(KB,2)+90.
    GO TO 67
60  S(LL)=TR
67  IF(LL-8)40,41,41
41  PUNCH 200,KL,(S(LL),LL=1,8)
    KL=KL+1
    LL=1
    GO TO 1
40  LL=LL+1
1   CONTINUE
    PUNCH 200,KL,(S(LL),LL=1,8)
    PAUSE
    IF(SENSE SWITCH 2)43,42
    END

C   DESCRIPTION OF SUBROUTINES
C   BRFRCB=BIREFRINGENCE OF CALCITE
C   BRFRQB=BIREFRINGENCE OF QUARTZ
C   FNOCB=REFRACTIVE INDEX ORDINARY RAY FOR CALCITE
C   FNOQB=REFRACTIVE INDEX ORDINARY RAY FOR QUARTZ
C   MATMPB=MATRIX MULTIPLICATION FOR 2X2 MATRIX WITH COMPLEX ELEMENTS
C         ONLY FIRST COLUMN IS COMPUTED
C   MATRXB=GENERATION OF S MATRIX

```

crystal. See Figure 1.) This changes Eq. (6) for γ according to Evans (1959) to:

$$\gamma = \pi d f(\epsilon, \omega, \varphi, \alpha) / \lambda \quad (12)$$

where

$$f = (\epsilon - \omega) \left\{ 1 - \frac{\varphi^2}{2\omega} \left(\frac{\cos^2 \alpha}{\omega} - \frac{\sin^2 \alpha}{\epsilon} \right) \right\}, \quad (13)$$

neglecting powers of φ equal to or higher than 4. The only change necessary in the computer program is to replace $(\epsilon - \omega)$ in Eq. (6) by the f defined in Eq. (13), and to add the computation of α for each birefringent plate.

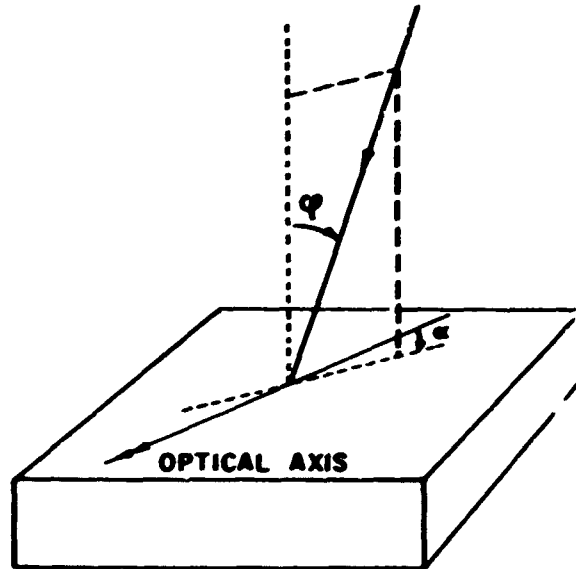


Figure 1. Definition of α and φ

Special cases of Eq. (13) are: for $\alpha = 0$ deg

$$f = (\epsilon - \omega) \left(1 - \frac{\varphi^2}{2\omega^2} \right), \quad (14)$$

and for $\alpha = 90$ deg

$$f = (\epsilon - \omega) \left(1 + \frac{\omega^2}{2\omega\epsilon} \right). \quad (14a)$$

This shows the well-known decrease in retardation for rays with $\alpha = 0$ deg and increase for those with an $\alpha = 90$ deg. For an α between these two extremes there is no change. This angle α_0 is given by Eq. (15):

$$\tan \alpha_0 = \left(\frac{\epsilon}{\omega} \right)^{1/2}. \quad (15)$$

2.3 Imperfect Polarizers

For reasons explained in Sec. 2.1, the computer program was written for a filter that starts with a perfect polarizer. In case the first polarizer is imperfect ($p_2 \neq 0$), the transmission may be found by computing the transmission T_1 of a filter with a perfect first polarizer and the transmission T_2 of a filter with a perfect first polarizer rotated over 90 deg with respect to the first one. The transmission of the filter, for unpolarized light, with the imperfect first polarizer can then be shown to be $p_1^2 T_1 + p_2^2 T_2$ or, since p_1 was always taken equal to 1, $T_1 + p_2^2 T_2$.

3. APPLICATIONS

3.1 Introduction

The ray-tracing program was used in four applications. In the first the on-axis transmission was determined for a birefringent filter of the Lyot type which was designed to operate at wavelengths of 3933.3, 6562.8 and 10,830.3 Å. Compromises were made in the thicknesses of the retardation plates in order to have the filter operate at these three wavelengths. Because of this, the filter will have leaks that are larger than those in a perfect Lyot filter at wavelengths away from the three main bands. The first application will assess the magnitude of these leaks. The angular field of Solc filters will be determined in the second application. So far, this angular field has not been determined theoretically. In the third application, the prediction made by Giovanelli and Jefferies (1954) on the improvement of the characteristics of the Lyot-filter transmission by using imperfect polarizers is checked and found true. The last application is concerned with the tolerances in plate thicknesses and angles required for satisfactory performance of Solc filters.

3.2 A Birefringent Filter for the Solar K, H_{α} , and He-10830 Lines

3.2.1 DESCRIPTION OF THE FILTER

3.2.1.1 Introduction

In the past the firm of Bernhard Halle Nachfl. of West Berlin has furnished several birefringent filters for the K line (3933 \AA). This filter is very sophisticated in that it involves a large number of elements; its $1/4$ and $1/2$ waveplates are made from two pieces of quartz with their optical axes crossed, and it has calcite-glass polarizers for high transmission in the ultraviolet. The filter is costly to build. Clearly, if such a filter could be used at more wavelengths than the K line (3933 \AA), [for instance, H_{α} (6563 \AA) and He I (10830 \AA)], its usefulness would be enhanced. All three of these wavelengths are of great interest to the solar astronomer. The line H_{α} is commonly observed with birefringent filters equipped with sheet polarizers. However, at present only comparatively wide passband birefringent filters have been used on prominences. A 10830 \AA filter requires calcite-glass polarizers.

We shall try to select a set of thicknesses for the K filter that will also work at the other wavelengths, preferably with no change in temperature. Such a solution means that the filter could be tested at H_{α} , which is in the visible and would never have to be checked in the infrared at He I.

3.2.1.2 Design Criteria

A number of design specifications must be met for this filter. Descriptions of these specifications are given below.

(1) Bandwidth

The bandwidth at the K line must be less than 0.15 \AA so that the K_2 peaks can be separated from the K_3 central emission. The passband of the He I line must be less than 1 \AA , preferably as narrow as 0.5 \AA , to ensure adequate contrast of solar detail on the solar disk. The H_{α} bandwidth must be less than 0.25 \AA , also to ensure adequate image contrast and good separation of the chromospheric images in the different parts of H_{α} .

Preliminary calculations showed that a 0.5 \AA element for the He I line would give 0.06 \AA at the K line, which is almost too narrow. Therefore, it was decided to separate the thickest calcite element from the rest of the filter.

Using the thick element, the final design gives a 0.20 \AA filter at the H_{α} line, 0.59 \AA at the He I line, and 0.06 \AA at the K line. Without this element the bandwidths are doubled.

(2) Tuning

It must be possible to tune the K-line filter at least $\pm 0.3 \text{ \AA}$ to obtain the K_2 peaks. To do this, at least three elements, and preferably four elements, in addition to the separable thickest element need to be tuned. The filter either must have

its elements immersed in oil with mechanical gearing to the tunable elements or it can be split into two more groups of elements, each of which has a tunable thick element at the ends. The latter approach was chosen for mechanical convenience and because the sun could be reimaged within each of the groups of elements so that more light flux could be transmitted. Furthermore, tuning all five of the thickest elements means that all the calcite elements are tuned and need not be made to any particular thickness. This is a great advantage since the indexes of calcite vary so much from piece to piece that it would be difficult to predict a solution for all three wavelengths.

A birefringent filter element is most easily tuned by adding a $1/4$ -wave plate to the element and then rotating the preceding polarizer. If one attempts this with calcite-glass prism polarizers the extra unused images begin to overlap in the image plane of the objective. One solution is to add $1/2$ -wave plates between the polarizer and $1/4$ -wave plates and rotate them. This is the solution that was chosen.

(3) Angular Field

In order to transmit as much light as possible the angular field of the filter must be as wide as possible. The simplest wide-field arrangement is to divide the element and insert a $1/2$ -wave plate in between. All the components must be properly oriented, of course. This is the method chosen for the filter. The elements can be made wide field until the thickest element again limits the angular field. If the thickest wide-field element has a field of $f/23$ (0.11 \AA at the K line), then there is no gain in making the 1.8 \AA quartz element wide field since it already has a field of $f/21$. Thus the five thickest elements must be wide field. The filter has fields of $f/23$ at the K line (0.114 \AA element) $f/22$ at the H_{α} line (0.2 \AA element) and $f/16$ at the He I line (0.59 \AA element).

(4) "Split-Element" Construction

In order to conserve polarizers the entire filter must be arranged with Evans' "split" elements. Here, a simple birefringent element is divided into two parts and placed on both sides of another element. The only criterion is that the polarizers must have their axes crossed, and that the order of the split element total an integer plus $1/2$. The order of the internal element may be an integer plus either $1/2$ or zero. In the former case the optical axes of the split components must be perpendicular, in the latter they must be parallel.

We must now choose the thicknesses for the elements of the filter that cannot easily be tuned. If we want to use the element for the outer plates of a "split" element, we must look for thicknesses of quartz whose order numbers exceed integers by $1/2$ for all three wavelengths at the same temperature. If we find a solution with integer orders for all three wavelengths, we may use this element as the central component in the "split" element.

A simple computer program was written to find all the thicknesses whose order number was coincident for the three wavelengths. Tolerances of 1/20th of an order were placed on each thickness. From this table we selected a set of thicknesses that were as near as possible to the 1 : 2 : 4 : 8 : ... ratio required for the simple birefringent filter. It was, of course, impossible to meet this requirement exactly since solutions do not exist. This is true for any split element filter since elements whose order is an integer plus 1/2 cannot add up in such a progression. The solution is indicated in Table 2 and Figure 2. The deviation from perfection can be estimated from studying the order numbers. It is, of course, only by chance that such a solution exists.

The results of the ray-tracing program to be described in Sec. 3.2.2 show that the chosen solution really contributed very little in parasitic light. The solution favors the K line because the center of the K line is only 4 percent of the continuum. Any parasitic light in the continuum is almost 25 times more detrimental than it would be at the He I line where there is no strong absorption line.

The E_1 element is required only if one wants to observe K and H_α simultaneously. It is not designed to work for He I. The E_4 element is the thickest, and necessary for He I. It would not really be required for K and H_α , although a narrow H_α filter is very useful.

(5) Waveplates

The waveplates pose a final problem. They must work at all three wavelengths. This may be accomplished by "achromatizing" the waveplates by using calcite combined with quartz. We did not investigate this method. We found that nature gave us a happy solution. For quartz a thickness of 1.50 orders at He I is almost exactly 2.50 at H_α and is almost exactly 4.50 at K. These higher order plates are used for 1/2-wave plates. The 1/4-wave plates use just half the thickness of these.

Using a high-order plate means that the waveplate will deviate more rapidly from 1/2 wave as one progresses away from the central peak. This is not serious because we plan to combine the filter with dielectric interference filters and because only the last five elements contain waveplates.

The ray-tracing program shows (Sec. 3.2.2) that the effect of high order waveplates is small. Since the waveplates are presently being made from two pieces of quartz anyway it is a simple matter to specify slightly different thicknesses and obtain a plate useful for all three wavelengths.

(6) Optical Arrangements

In order to transmit as much flux as possible we image the sun inside of each of the large sections E_2 , E_3 , and E_4 . A field lens, cemented to the end of each

Table 2. Composition of the Filter for the K, H α , and He I Line

ELEMENT	ORIENTATION (DEGREES)	THICKNESS (MM.)	RETARDATION		
			3933.68 Å	6562.81 Å	10830.3 Å
ELEMENT E1					
POLARIZER	0.0				
QUARTZ	45.0	.565250	13.746	7.752	4.541
QUARTZ	0.0	2.261000	54.987	31.010	18.164
QUARTZ	45.0	.565250	13.746	7.752	4.541
POLARIZER	90.0				
QUARTZ	45.0	2.313500	56.264	31.730	18.585
QUARTZ	0.0	.657000	15.978	9.011	5.278
QUARTZ	45.0	2.313500	56.264	31.730	18.585
ELEMENT E2					
POLARIZER	0.0				
QUARTZ	VAR.	.164000	4.474	2.523	1.478
QUARTZ	0.0	.092500	2.249	1.268	.743
CALCITE	45.0	14.186000	6693.213	3664.493	2124.504
QUARTZ	0.0	.184000	4.474	2.523	1.478
CALCITE	315.0	14.186000	6693.213	3664.493	2124.504
POLARIZER	0.0				
QUARTZ	45.0	18.390500	447.256	252.235	147.742
QUARTZ	0.0	4.048000	98.447	55.520	32.520
QUARTZ	315.0	18.390500	447.256	252.235	147.742
POLARIZER	90.0				
CALCITE	45.0	7.093000	3346.606	1832.246	1062.252
QUARTZ	0.0	.184000	4.474	2.523	1.478
CALCITE	315.0	7.093000	3346.606	1832.246	1062.252
QUARTZ	0.0	.092500	2.249	1.268	.743
QUARTZ	VAR.	.184000	4.474	2.523	1.478
POLARIZER	0.0				
ELEMENT E3					
QUARTZ	VAR.	.184000	4.474	2.523	1.478
QUARTZ	0.0	.092500	2.249	1.268	.743
CALCITE	45.0	3.546500	1673.303	916.123	531.126
QUARTZ	0.0	.184000	4.474	2.523	1.478
CALCITE	315.0	3.546500	1673.303	916.123	531.126
POLARIZER	0.0				
QUARTZ	45.0	4.574500	111.251	62.741	36.749
QUARTZ	0.0	18.114000	440.532	248.442	145.520
QUARTZ	315.0	4.574500	111.251	62.741	36.749
POLARIZER	90.0				
QUARTZ	315.0	36.873500	896.762	505.738	296.227
QUARTZ	0.0	.184000	4.474	2.523	1.478
QUARTZ	45.0	36.873500	896.762	505.738	296.227
QUARTZ	0.0	.092500	2.249	1.268	.743
QUARTZ	VAR.	.184000	4.474	2.523	1.478
POLARIZER	0.0				

Table 2 (Continued)

ELEMENT E4					
QUARTZ	VAR.	.184000	4.474	2.523	1.478
QUARTZ	0.0	.092500	2.249	1.268	.743
CALCITE	45.0	28.372000	13386.426	7328.986	4249.009
QUARTZ	0.0	.184000	4.474	2.523	1.478
CALCITE	315.0	28.372000	13386.426	7328.986	4249.009
POLARIZER	0.0				

OPERATING TEMPERATURE = 42.0 DEGREES C.

element, forms an image of the objective on a diaphragm. Because the calcite-glass polarizers do not absorb any light, there will be a large number of images of the objective present. The desired one must be selected by the diaphragm. The deviation of the polarizers needs only to be equal to the angular field of the filter.

At each diaphragm there will be a reimaging lens that will form an image of the sun inside of the next group of elements. Finally, before each group of elements there must be another field lens that collimates the diaphragm so that the axis of each cone of light to every point in the field is parallel. This ensures uniform spectral transmission over the field. It may be necessary to add a field flattener to take out the curvature of field introduced by the field lenses.

Considering the expansion inside of each element using the maximum angular field of the filter, the useful field aperture is about 26 mm for a 30-mm clear-filter aperture. To photograph the entire sun one could use a 5-in. diam objective for K and H_{α} and a 7-in. diam objective for He I.

3.2.2 TRANSMISSION OF THE FILTER

The transmission profiles of this filter are determined for 200 Å intervals centered on the K, H_{α} , and He I lines. In order to measure all the details of these transmission profiles one has to compute the transmission profiles at wavelength intervals that are a fraction of the halfwidth of the main transmission band of the filter. In the present calculation this fraction is taken as approximately 1/3. The results for the three transmission bands follow.

3.2.2.1 The K Line (3933.68 Å)

For the observation of this line the elements E_1 , E_2 , and E_3 will be used giving a halfwidth of the main transmission band of 0.114 Å. The transmission is calculated at 0.04 Å intervals. The directions of the tunable $\lambda/2$ plates are taken such that the main band is centered on the K line. These orientations are given in Table 3. (Orientation is given with respect to the first polarizer, positive when

clockwise in Figure 2.) Figure 3 gives the transmission profile for this filter. The transmission at maximum is 90.6 percent. This result disregards light losses due to reflection and absorption. The deviations from a perfect filter are very small on the K line because many of the retardation plate thicknesses were taken close to the theoretical value for K and because the adjustment of the calcite plate thicknesses to those for quartz was best for K.

From the graphs given in Figure 3 we determined the total amount of parasitic light (light in secondary maxima) in various intervals around the main band. This amount, expressed in the total transmission of the main band, is given in Table 4 for both an equi-energy density spectrum passing through the filter (T_p/T_m) and for a solar absorption line spectrum (I_p/I_m) passing through the filter. The data in Table 4 are also given in Figures 5 and 6.

Table 3. Orientations of the $\lambda/2$ Plates for the K-Line Filter

$\lambda/2$ Plate Number	Orientation
1	51.8°
2	64.1°
3	35.5°
4	2.3°

Table 4. Relative Amount of Parasitic Transmissions for Bands of Various Widths Centered on the K-Line

Bandwidth (Å)	T_p/T_m (%)	I_p/I_m (%)
2	11.2	25
4	12.5	28
8	13.4	35
13	13.5	36
32	13.6	38
64	13.8	42
128	13.9	46

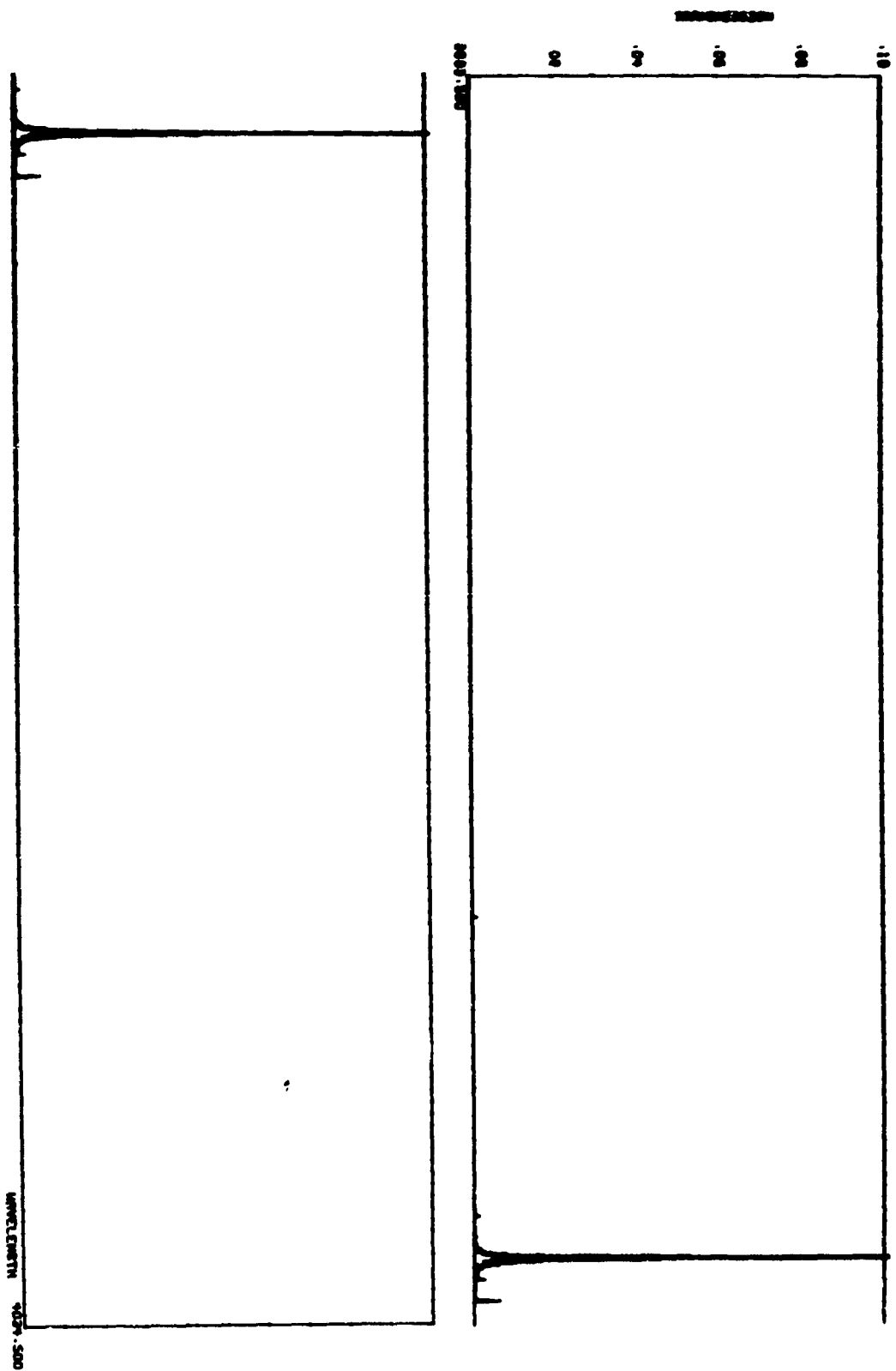


Figure 3. On-Axis Transmission of Three-Line Filter at K (3933.3 \AA). Elements E1, E2, and E3

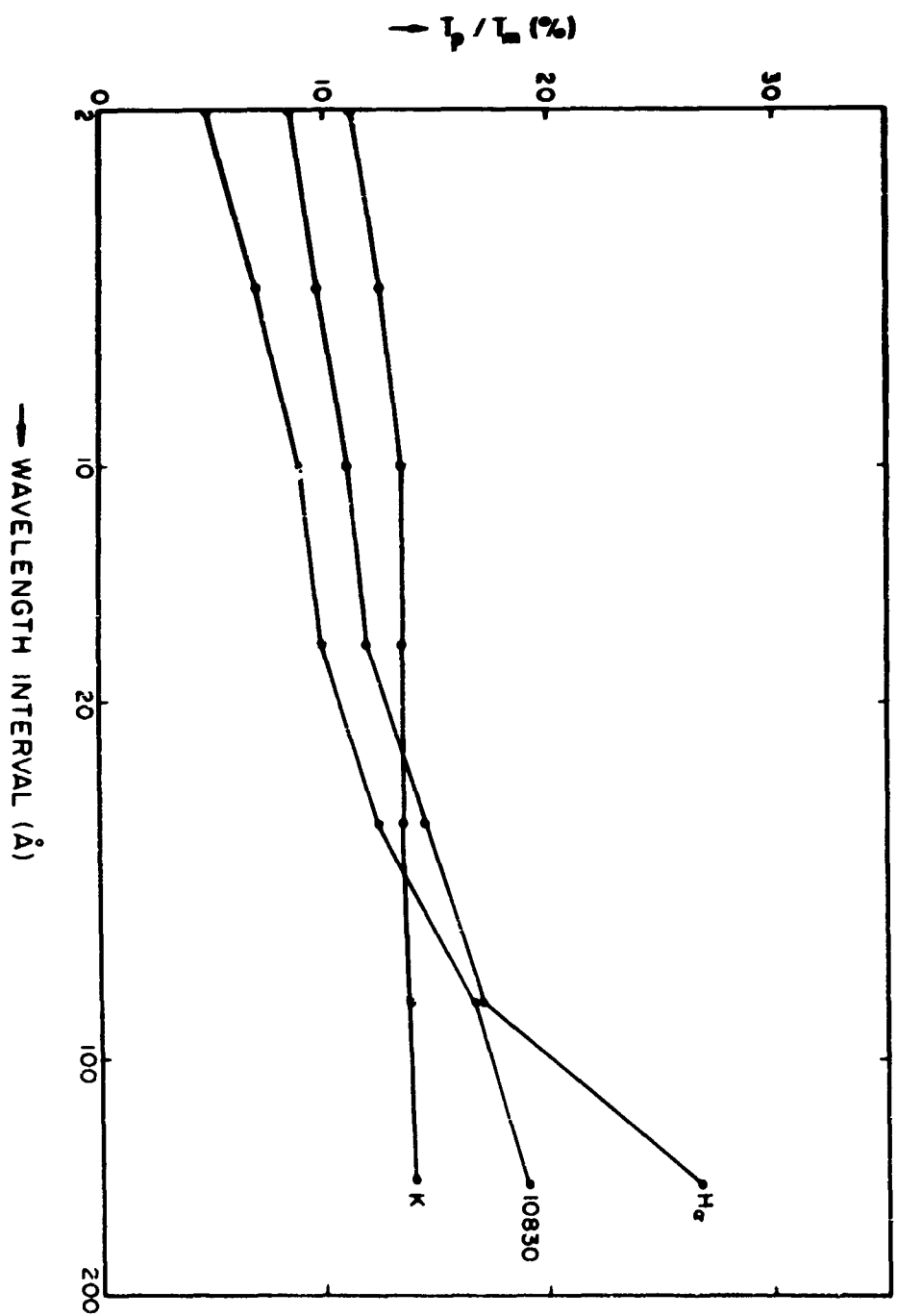


Figure 5. Integrated Parasitic Transmission T_p for Various Wavelength Intervals Centered on the Principal Wavelength Expressed in the Transmission of the Main Band T_m

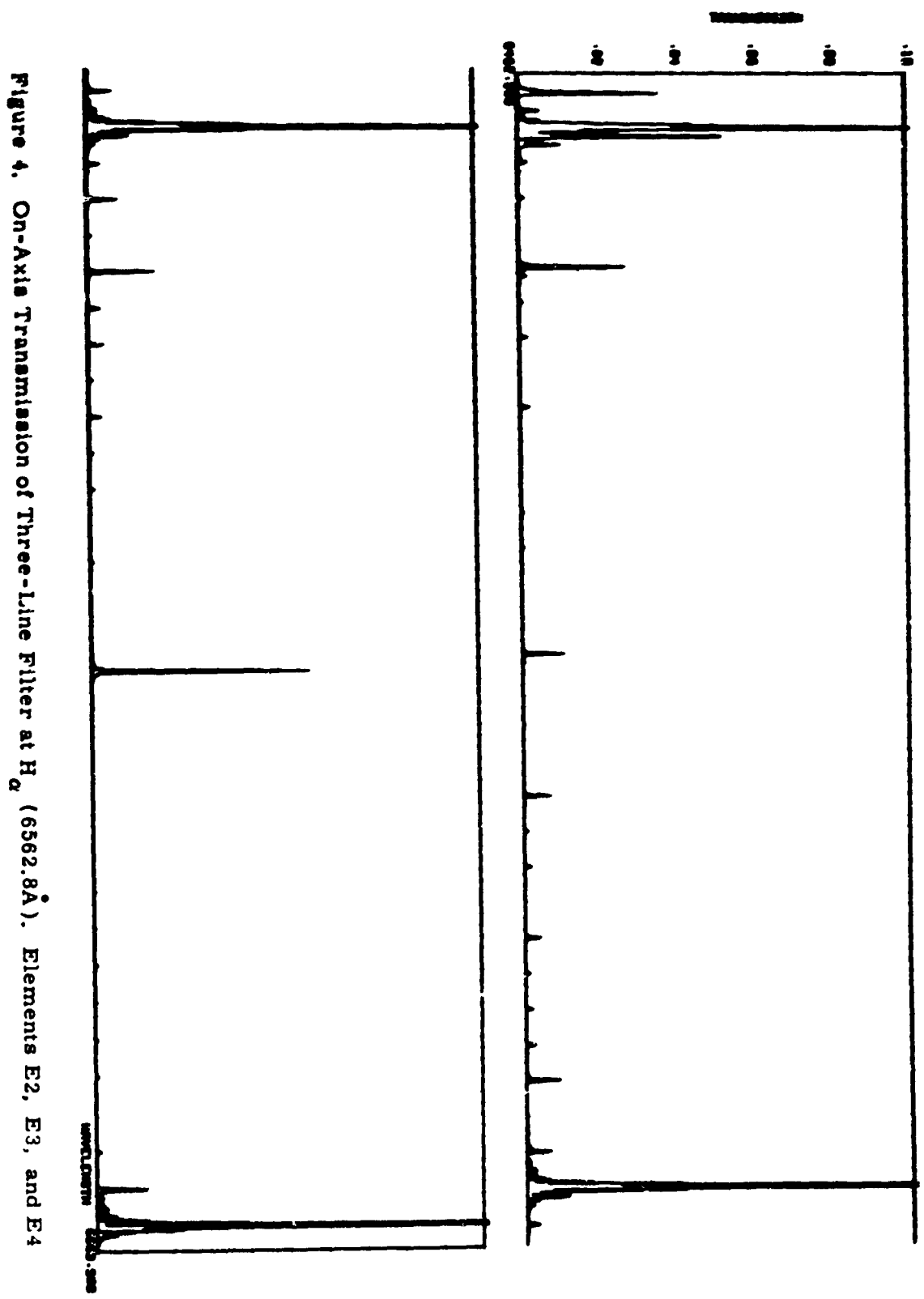


Figure 4. On-Axis Transmission of Three-Line Filter at H_{α} (6562.8 Å). Elements E2, E3, and E4

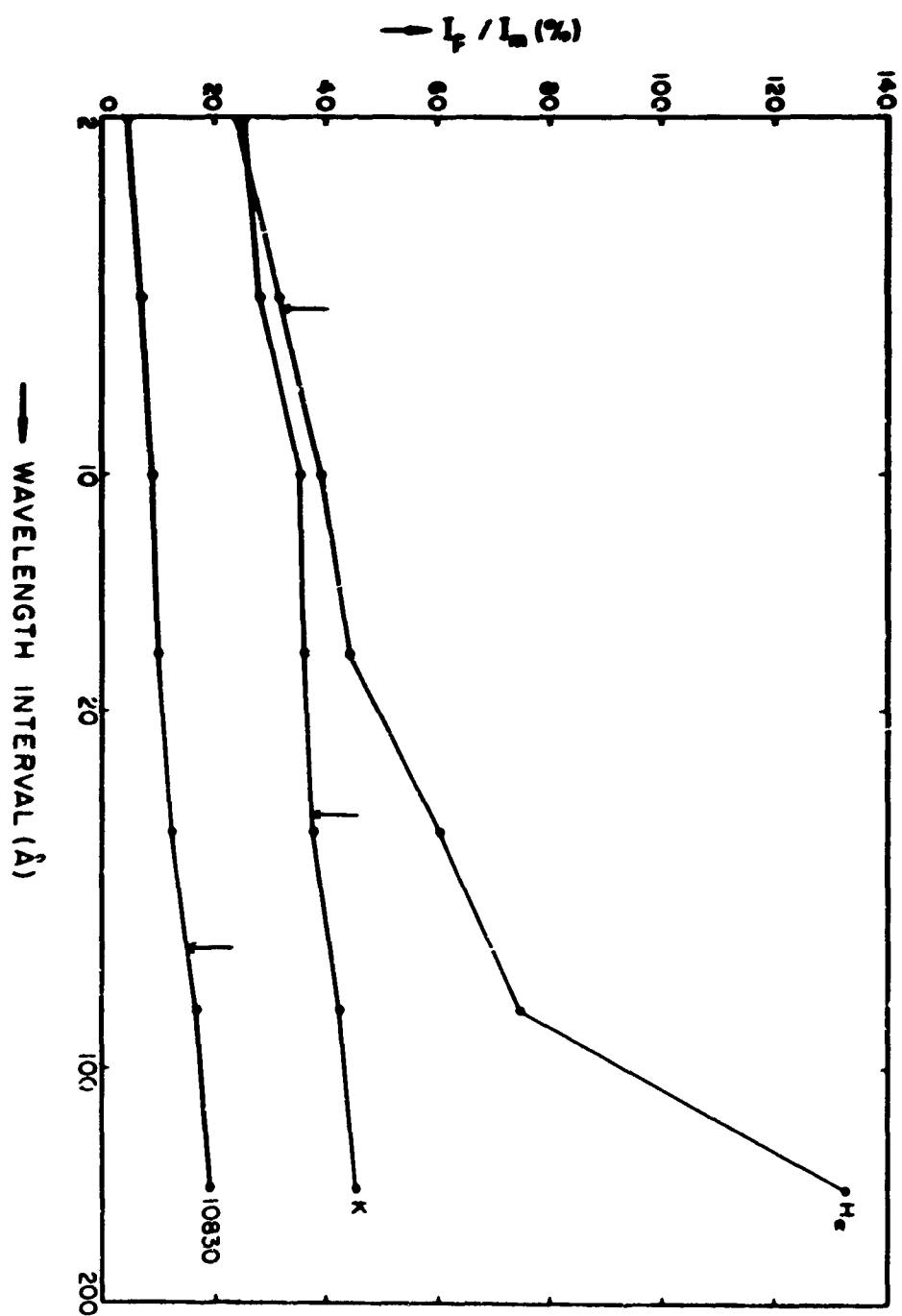


Figure 6. Integrated Parasitic Intensities I_p for Various Wavelength Intervals Centered on the Principal Wavelengths Expressed in the Intensity of the Main Band I_m . The arrows indicate the halfwidth of available blocking-interference filters for each wavelength

3.2.2.2 The H_{α} Filter (6562.81 Å)

Computations were made for a filter composed of elements E_2 , E_3 , and E_4 , which together give a halfwidth of the main transmission of 0.202 Å. The transmission is calculated for intervals of 0.08 Å. Table 5 gives the orientations of the $\lambda/2$ plates so that the main band is centered on H_{α} . Figure 4 gives the transmission profile of this filter. The transmission at maximum is 93.4 percent, again omitting losses due to reflections and absorptions. The strong bands about 95 Å away from H_{α} are the next main filter maxima transmitted by the thinnest plate in the filter. The many secondary maxima in between are due to the imperfect matching of the retardation plates. Table 6 and Figures 5 and 6 again give T_p/T_m and I_p/I_m . The increased amount of parasitic transmission is not as serious as it would have been if it had been near the K line, because the H_{α} line in the solar spectrum is weaker than the K line. The availability of better blocking (interference) filters near H_{α} makes the amount of parasitic transmission tolerable.

Table 5. Orientation of $\lambda/2$ Plates for the H_{α} Filter

$\lambda/2$ Plate Number	Orientation
1	1.2°
2	69.4°
3	67.8°
4	88.4°
5	2.3°

Table 6. Relative Amount of Parasitic Transmissions for Band of Various Widths Centered on the H_{α} Line

Bandwidth (Å)	T_p/T_m (%)	I_p/I_m (%)
2	8.5	25
4	9.7	32
8	11.0	39
16	11.9	44
32	14.5	60
64	17.1	75
128	26.8	133

3.2.2.3 The He-I Filter (10,830.3 Å)

For this line, the elements E_2 , E_3 , and E_4 will again be used giving a half-width of the main transmission band of 0.59 Å. Calculations of the transmissions were made at intervals of 0.20 Å. Table 7 again gives the directions of the $\lambda/2$ plates. Figure 7 shows the transmission profile of the filter. Omitting absorption and reflection losses, peak transmission is 94.8 percent. The solar spectrum at this wavelength is practically void of absorption lines so that $T_p/T_m \approx I_p/I_m$. Table 3 and Figures 5 and 6 give these quantities.

Table 7. Orientation of $\lambda/2$ Plates for the He-10830 Line

$\lambda/2$ Plate Number	Orientation
1	89.1°
2	0.4°
3	67.3°
4	4.0°
5	88.2°

Table 8. Relative Amount of Parasitic Transmissions for Bands of Various Widths Centered on the He-10830 Line

Bandwidth (Å)	T_p/T_m (%) = I_p/I_m (%)
2	4.8
4	7.0
8	9.0
16	9.9
32	12.4
64	16.7
128	19.1

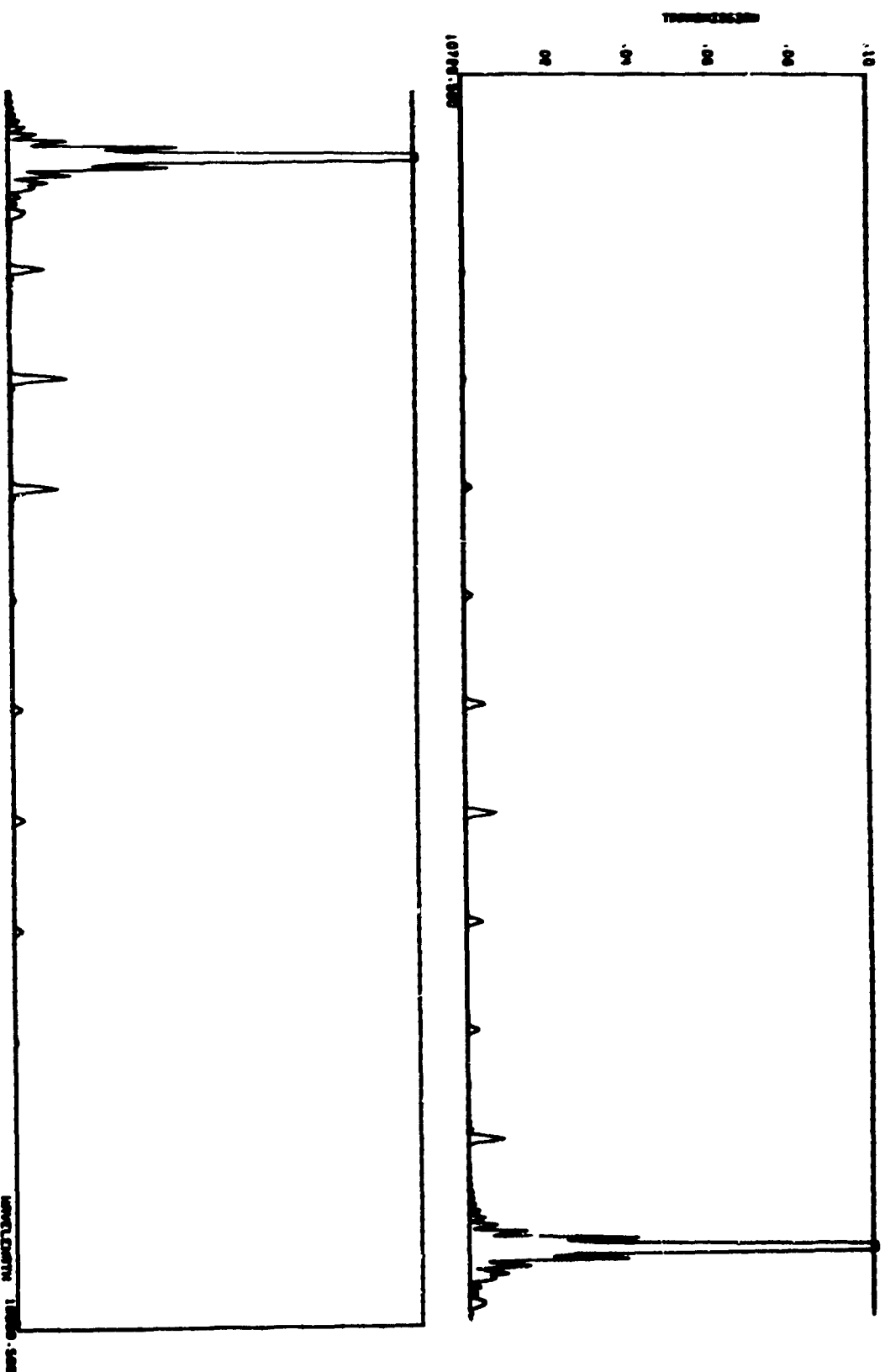


Figure 7. On-Axis Transmission of Three-Line Filter at He-10830. Elements E₂, E₃, and E₄

3.2.3 CONCLUSIONS

As the filter will be used with sunlight, one has to consider values of I_p/I_m when assessing the parasitic light. Introduction of parasitic light will reduce the contrast of the structures that are normally visible only in the three lines. This reduction of contrast is equal to $1 + I_p/I_m$. If one considers a contrast reduction of a factor 2 tolerable, I_p/I_m may be as much as 100 percent. The actual magnitude of I_p/I_m will be determined by the properties of the blocking filters used with the filter. The important quantity is the halfwidth of the transmission profiles of these filters. In order to make I_p/I_m small, interference filters will have to be used with a narrow transmission profile. An approximate value of I_p/I_m can be obtained by reading the graph of Figure 6 at a bandwidth equal to the halfwidth of the filter. The halfwidths of three filters which are currently available are indicated in Figure 6. Filters of still smaller halfwidth are available, but are not plotted because of their low peak transmission. The highest I_p/I_m occurs for the K line. It is 38 percent which we consider to be tolerable. In contrast, the resulting reduction is 1.38.

3.3 Off-Axis Characteristics of Solc Filters

3.3.1 DESCRIPTION OF THE VARIOUS FILTERS USED

In his papers, Solc (1959, 1960) describes four types of filters, all of which use a pile of equal-thickness retardation plates between two polarizers. The four types distinguish themselves by the orientations of the retardation plates and polarizers. In the first type, which we will call type A, all plates make equal angles ϵ with the direction of the first polarizer, but alternate between plus and minus ϵ . This type was called the folded filter by Evans (1958). The ϵ is equal to $45 \text{ deg}/N$ where N is the number of plates. The thickness of the plates is such that the retardation at the wavelength of peak transmission is an integer $+1/2$. The last polarizer has to be at right angles to the first one. Table 9 lists a filter of this type that we have tested by computation. In the second type filter (B), the plates also make angles of 2ϵ with each other, but are now arranged in a fan with the first plate making an angle of ϵ with the first polarizer. The last polarizer is now parallel to the first one. The retardation of each plate, in this case, is an integer for the wavelength of the transmission peaks. Table 10 lists such a filter (Solc B). It is the equivalent of the Solc A listed in Table 9 and contains the same number of plates.

Evans (1958) computed the transmission of these two types of filters. He showed that these transmissions are the same for filters of types A and B for an equal number of elements. He also found these first two types of Solc filters to be inferior to the Lyot filter in the suppression of parasitic light. The curves in

Table 9. Composition of the Solc-A Filter*

Element	Orientation (deg)	Thickness (mm)	Retardation (6563.73 Å)
Polarizer	0		
Calcite	3	1.546787	399.5
Calcite	357	1.546787	399.5
Calcite	3	1.546787	399.5
Calcite	357	1.546787	399.5
Calcite	3	1.546787	399.5
Calcite	357	1.546787	399.5
Calcite	3	1.546787	399.5
Calcite	357	1.546787	399.5
Calcite	3	1.546787	399.5
Calcite	357	1.546787	399.5
Calcite	3	1.546787	399.5
Calcite	357	1.546787	399.5
Calcite	3	1.546787	399.5
Calcite	357	1.546787	399.5
Calcite	3	1.546787	399.5
Polarizer	90		

Table 10. Composition of the Solc-B Filter*

Element	Orientation (deg)	Thickness (mm)	Retardation (6563.73 Å)
Polarizer	0		
Calcite	3	1.548723	400
Calcite	9	1.548723	400
Calcite	15	1.548723	400
Calcite	21	1.548723	400
Calcite	27	1.548723	400
Calcite	33	1.548723	400
Calcite	39	1.548723	400
Calcite	45	1.548723	400
Calcite	51	1.548723	400
Calcite	57	1.548723	400
Calcite	63	1.548723	400
Calcite	69	1.548723	400
Calcite	75	1.548723	400
Calcite	81	1.548723	400
Calcite	87	1.548723	400
Polarizer	0		

* Operating Temperature = 42.0°C

Figure 8 give the transmission for the Solc A and B filters as listed in Tables 9 and 10 as well as the one for an equivalent Lyot filter. Later, by altering the orientation of the optical axes of the birefringent plates, Solc managed to suppress the secondaries very effectively at the cost of increasing the width of the main maximum. By adding a few plates, this width could be reduced again so that a filter actually was obtained with a lower amount of parasitic light than the Lyot filter but with equal halfwidth. These altered orientations of the plates are defined in Solc (1960, 1965) papers. Tables 11 and 12 list two such filters. The first, a modification of the folded filter, will be called the Solc-C filter; the second, a modified fan filter, is called the Solc-D filter. The number of plates is taken to give approximately the same width as the Solc-A or Solc-B filters and the Lyot filter given in Figure 8. Figure 8 shows the transmission profile of the Solc-C and Solc-D filters as well (the two are identical). The parasitic transmission is indeed much lower than that for the Lyot filter.

Table 11. Composition of the Solc-C Filter

Element	Orientation (deg)	Thickness (mm)	Retardation (6563.73 Å)
Polarizer	0.0		
Calcite	1.5	1.546787	399.5
Calcite	358.2	1.546787	399.5
Calcite	2.0	1.546787	399.5
Calcite	357.7	1.546787	399.5
Calcite	2.5	1.546787	399.5
Calcite	357.2	1.546787	399.5
Calcite	3.0	1.546787	399.5
Calcite	356.7	1.546787	399.5
Calcite	3.5	1.546787	399.5
Calcite	356.5	1.546787	399.5
Calcite	3.2	1.546787	399.5
Calcite	357.0	1.546787	399.5
Calcite	2.7	1.546787	399.5
Calcite	357.5	1.546787	399.5
Calcite	2.2	1.546787	399.5
Calcite	358.0	1.546787	399.5
Calcite	1.7	1.546787	399.5
Calcite	358.5	1.546787	399.5
Polarizer	90.0		

Operating Temperature = 42.0°C

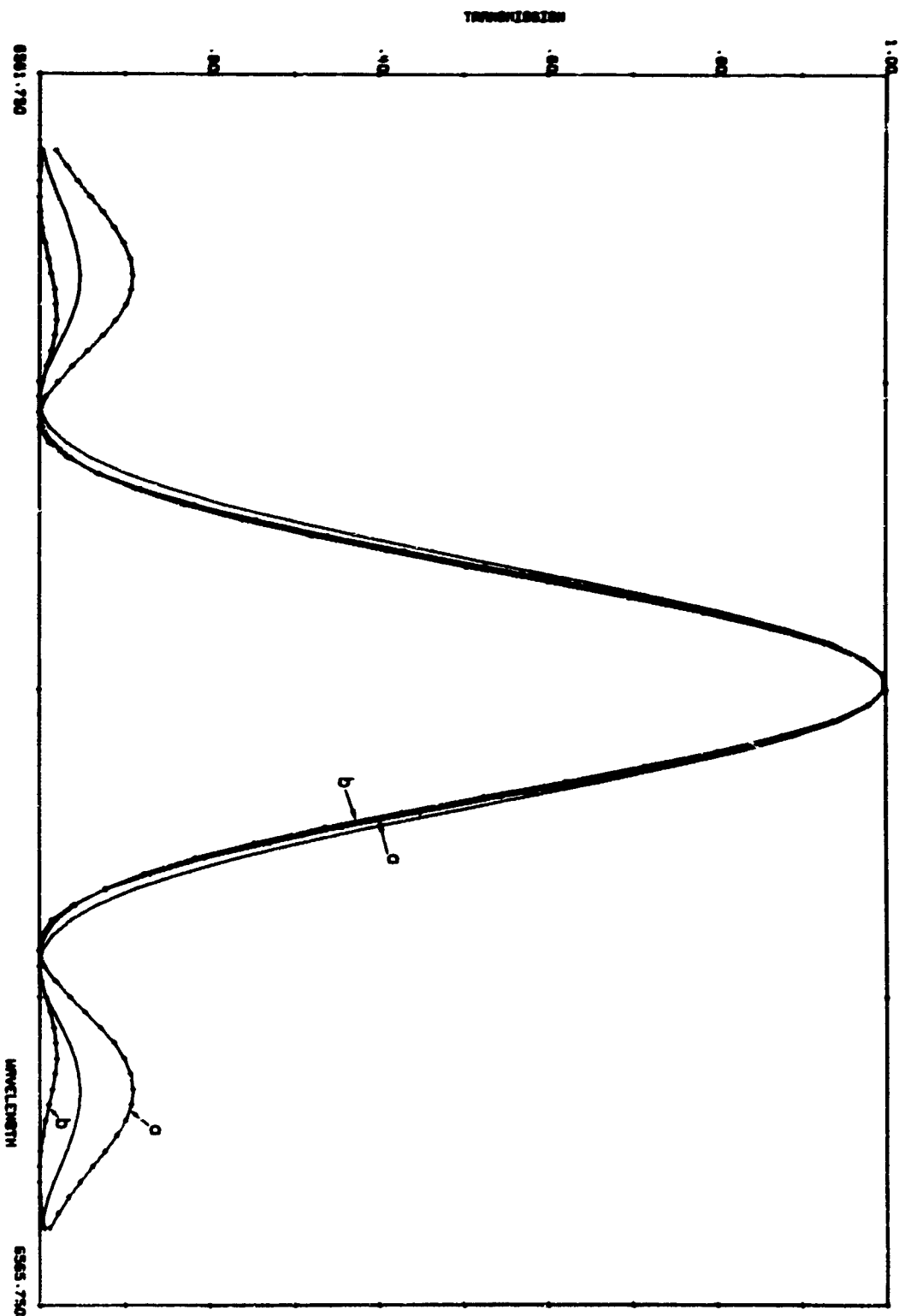


Figure 8. On-Axis Transmission of Two Types of Solc Filters (dashed line) as Compared with a Comparable Lyot Filter (solid line). (a) Type A or B Filter, (b) Type C or D Filter

Table 12. Composition of the Šolc-D Filter

Element	Orientation (deg)	Thickness (mm)	Retardation (6563.73 Å)
Polarizer	0.0	1.548723	400
Calcite	1.5	1.548723	400
Calcite	4.7	1.548723	400
Calcite	8.5	1.548723	400
Calcite	12.7	1.548723	400
Calcite	17.5	1.548723	400
Calcite	22.7	1.548723	400
Calcite	28.5	1.548723	400
Calcite	34.7	1.548723	400
Calcite	41.5	1.548723	400
Calcite	48.7	1.548723	400
Calcite	55.5	1.548723	400
Calcite	51.7	1.548723	400
Calcite	67.5	1.548723	400
Calcite	72.7	1.548723	400
Calcite	77.5	1.548723	400
Calcite	81.7	1.548723	400
Calcite	85.5	1.548723	400
Calcite	89.7	1.548723	400
Polarizer	0.0		

Operating Temperature = 42.0°C

3.3.2 TRANSMISSION FOR OFF-AXIS RAYS

In his papers, Šolc points out that the off-axis behavior is similar to that for a non-wide-angle Lyot filter. This can easily be understood for a Šolc-A or -C filter, but not for a Šolc-B or -D filter. In order to examine the off-axis properties more closely, the transmission profiles of the filters described in Sec. 3.3.1 were determined for a ray incident at 1 deg to the normal at azimuths (α) (see Sec. 2.2) of 0.0, 22.5, 45.0, 67.5, 90.0, 112.5, 135.0, and 157.5 deg. Table 13 gives the resulting wavelength shift of the main transmission peak with respect to the peak position for on-axis rays. It shows that the maximum displacements for Šolc-B and -D filters are approximately 20 percent less than those for the Šolc-A and -C filters, which results in a 10 percent increase in usable angular aperture for the B and D filters. The Šolc-B and -D filters have a larger usable angular aperture than the Lyot filters.

An altered version of the C filter was also computed. This version, called Šolc CC, inserts a "rotator" between the ninth and tenth element of the filter. This "rotator" rotates the direction of polarization of incident light 90 deg or, more exactly, rotates the Poincaré sphere 180 deg around the axis that is at right angles to the circle of perfect polarized light. In the Jones calculus (1941), such a rotator is represented by the matrix

Table 13. Shift of Transmission Band in Angstroms for Off-Axis Rays Incident at 1 deg to the Normal for Five Types of Solc Filters. The peak wavelength is near 6563 Å

Azimuth (deg)	Solc A	Solc B	Solc C	Solc D	Solc CC
0	-0.33	+0.02	-0.33	+0.02	+0.01
22.5	-0.23	-0.18	-0.23	-0.17	+0.02
45	+0.02	-0.26	+0.02	-0.25	+0.02
67.5	+0.26	-0.13	+0.26	-0.17	+0.02
90	+0.36	+0.02	+0.36	+0.02	+0.01
112.5	+0.26	+0.22	+0.26	+0.21	+0.02
135	+0.02	+0.29	+0.02	+0.28	+0.02
157.5	-0.23	+0.22	-0.23	+0.21	+0.02
180	-0.33	+0.02	-0.33	+0.02	+0.01

$$\begin{pmatrix} 0 & 1 \\ -1 & 0 \end{pmatrix} \quad (16)$$

which can be inserted into Eq. (7) at the appropriate location. By rotating all the elements of the filter on one side of this rotator (including the polarizer) 90 deg, one then obtains a filter that has the same on-axis transmission characteristics as the original filter. In this modified filter the axes of the birefringent plates are crossed so that one may expect an increase of the filter's usable aperture as in the case of the Lyot filter. Table 14 lists the elements of this wide-angle modification of the Solc-C filter. Two quartz $\lambda/2$ plates placed 45 deg to each other act here as the 90-deg rotator. The last column of Table 13 gives the computed off-axis displacements for this filter. There is indeed an improvement of a factor of about 16, or of a factor 4 in the diameter of the usable aperture. For a filter with quartz elements, this factor presumably will be even better, as is the case for a Lyot filter.

The displacement of the transmission band is, however, not the only criterion that defines the usable filter aperture. Another requirement is that the transmission profile within this aperture does not change too much from that for the on-axis rays. This requirement is not fulfilled for the types B, D, and CC Solc filters. It will be shown in Sec. 3.5 that the retardation of the individual plates in Solc filters has to be the same within very close tolerances. When this is not the case, a serious deterioration of the transmission profile results. The retardation changes rapidly for off-axis rays in the types B, D, and CC filters due to the large changes in the azimuth α . The result is a poor transmission profile. On the other hand, the changes in α are small for types A and C filters, hence the good off-axis profiles. Figure 9 shows two examples for off-axis profiles with types CC and

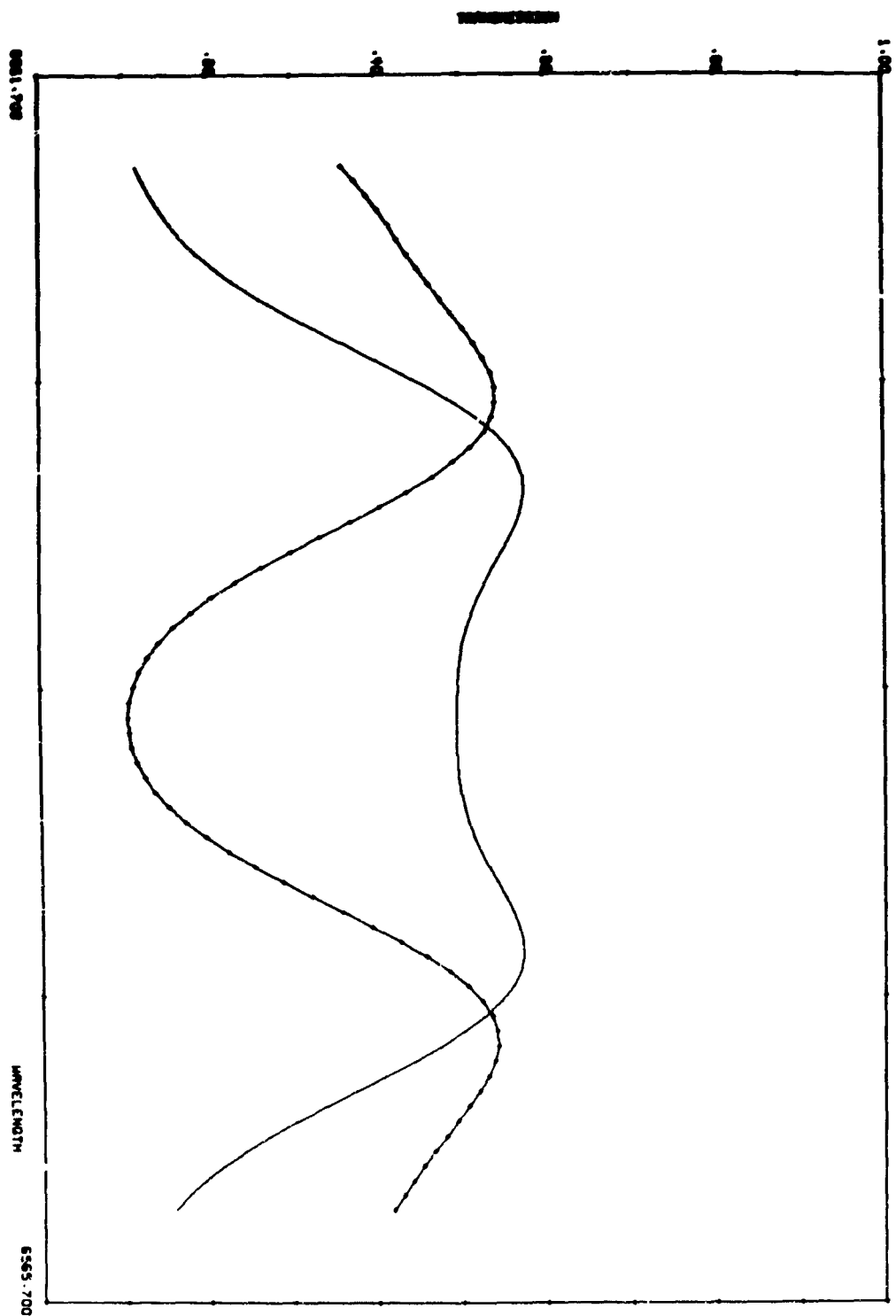


Figure 9. Off-Axis Transmission Profile of a Solc-D Filter ($\phi = 2.0$ deg, $\alpha = 0$ deg) (solid line) and of a Solc-CC Filter ($\phi = 2.0$ deg, $\alpha = 0$ deg) (dashed line)

Table 14. Composition of the Šolc-CC Filter

Element	Orientation (deg)	Thickness (mm)	Retardation (6563.73 Å)
Polarizer	0.0		
Calcite	1.5	1.546787	399.5
Calcite	358.2	1.546787	399.5
Calcite	2.0	1.546787	399.5
Calcite	357.7	1.546787	399.5
Calcite	2.5	1.546787	399.5
Calcite	357.2	1.546787	399.5
Calcite	3.0	1.546787	399.5
Calcite	356.7	1.546787	399.5
Calcite	3.5	1.546787	399.5
Quartz	22.5	0.036454	0.5
Quartz	67.5	0.036454	0.5
Calcite	86.5	1.546787	399.5
Calcite	93.2	1.546787	399.5
Calcite	87.0	1.546787	399.5
Calcite	92.7	1.546787	399.5
Calcite	87.5	1.546787	399.5
Calcite	92.2	1.546787	399.5
Calcite	88.0	1.546787	399.5
Calcite	91.7	1.546787	399.5
Calcite	88.5	1.546787	399.5
Polarizer	0.0		

D filters. For both curves the wavelength displacement is tolerable, but the profile deterioration is not.

The folded Šolc filters are definitely superior to the fan filters in off-axis transmission. A simple wide-angle configuration, as tried above for the type CC filter, is not usable because of the profile deterioration for off-axis rays. One probably has to go to the laborious work of making each individual element of a Šolc filter a wide-angle element, as is normally done in a Lyot filter, in order to obtain a wide-angle Šolc filter (Šolc, 1959).

3.4 Lyot Filters with Imperfect Polarizers

Giovanelli and Jefferies (1954) analyzed the influence of the use of imperfect polarizers on the performance of Lyot filters. They came to the surprising result that a slight imperfection of the polarizers can actually improve the performance of the Lyot filter if this performance is defined as the ratio of the total transmission T_m in the main filter band between the first minima on either side to the total transmission in the secondaries T_p .

From the same paper we used the following equations for the ratio T_p/T_m :

$$T_p/T_m = 0.11 + 0.61 p_2 + N p_2^2 \quad (17)$$

for a filter with N plates whose retardation directions are parallel (to be called the "parallel filter"), and

$$T_p/T_m = 0.11 - 0.61 p_2 + N p_2^2 \quad (17a)$$

for a filter in which the retardation direction of each plate is perpendicular to that of its immediate predecessor (the "crossed filter"). The term p_2 has been defined in Sec. 2.1 as the square root of the ratio of the intensity transmittances of the polarizer for light polarized in the unwanted and wanted directions. Equation (17) shows that, for the parallel filter, T_p/T_m increases for increasing p_2 thereby deteriorating the filter performance. From Eq. (17a), it follows that, for the crossed filter, T_p/T_m first decreases with increasing p_2 and only starts to increase for larger values of p_2 . The ratio T_p/T_m is minimum when $p_2 \neq 0$ at

$$p_2 = 0.305/N. \quad (18)$$

This means that the use of high-transmission polaroid polarizers which, consequently, have a rather large cross transmission p_2 will not only improve the absolute transmission at the primary peak but will also suppress, in relative importance, the parasitic transmissions.

Since this result was viewed skeptically by many, we decided to verify it with the present ray-tracing program. A four-element Lyot filter which had a 1 \AA halfwidth near 6563 \AA was examined. The optimum p_2 for this filter, according to Eq. (18), is 7.6 percent. The transmission was then computed for a filter with $p_2 = 0$ percent, and for a parallel and crossed filter with $p_2 = 7.6$ percent. The top portion of Figure 10 shows the resulting transmission profile for the $p_2 = 0$ percent filter, and the bottom portion shows the differences in transmission from this profile for the parallel and the crossed filter. It is indeed clear from Figure 10 that the transmission in the main band is increased for the crossed filter while there is a small decrease in the parasitic transmissions. The opposite is true for the parallel filter, so there is at least a qualitative agreement with the prediction. The difference in T_p/T_m between the $p_2 = 7.6$ percent and $p_2 = 0$ percent filters was also determined with the following results:

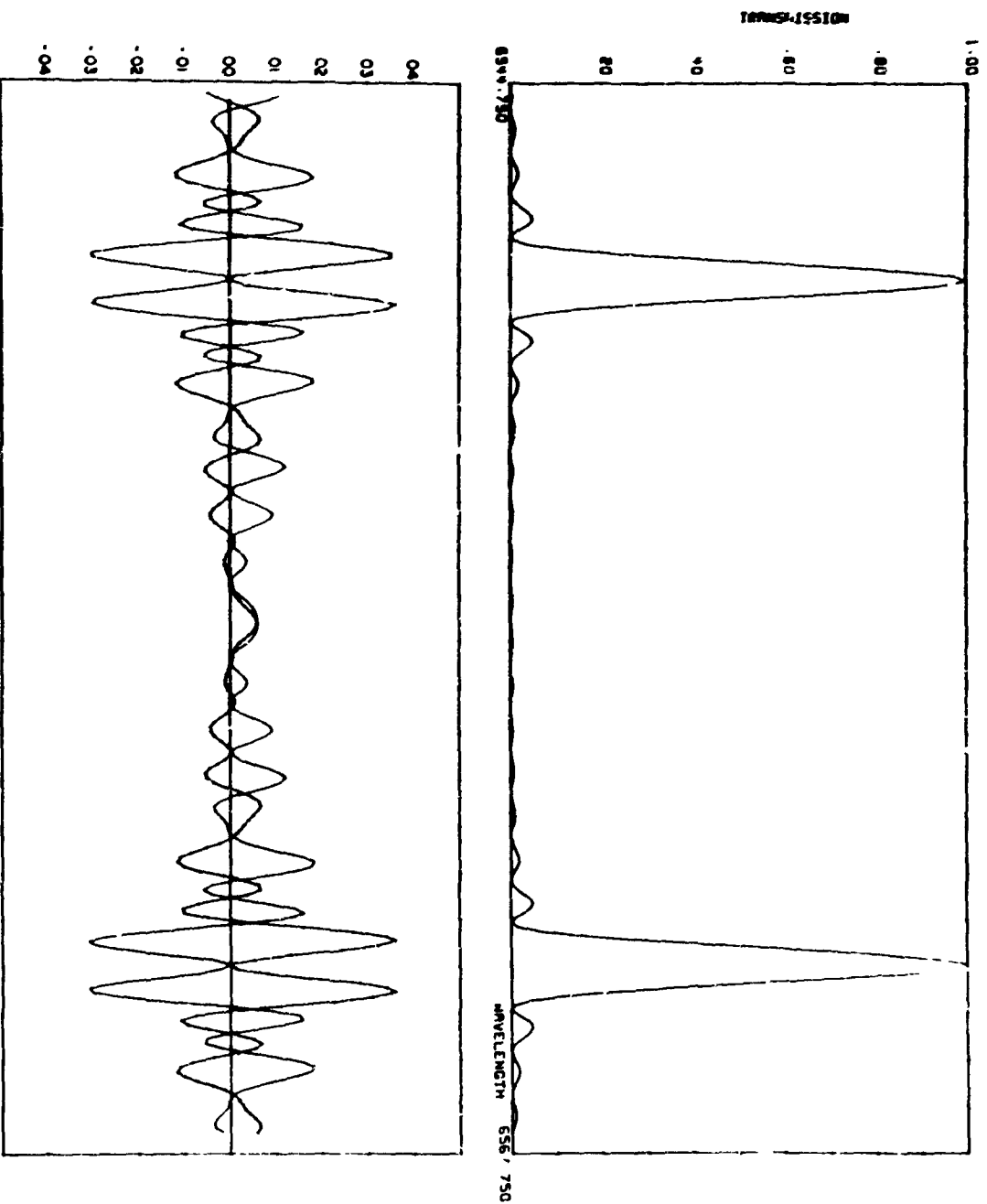


Figure 10. The Effect of Imperfect Polarizers on 4-Element On-Axis Lyot Filter Transmission. Top Graph: Lyot filter transmission with perfect polarizers. Lower graph: difference of Lyot filter transmission with imperfect polarizers from that for imperfect polarizers for a crossed (dashed line) and parallel (solid line) filter

$$\Delta(T_p/T_m) = +0.074$$

for the parallel filter, and

$$\Delta(T_p/T_m) = -0.016$$

for the crossed filter in reasonable agreement with the values predicted from Eqs. (17) and (17a) which give +0.070 and -0.023, respectively.

The prediction by Giovanelli and Jefferies is correct. In the design of Lyot filters this property should be kept in mind since the use of imperfect polarizers often could result in a greatly improved transmission of the filter.

3.5 Tolerances for Solc Filters

3.5.1 INTRODUCTION

In this section we will examine the tolerances that are required on the thicknesses and orientations of the retardation plates in a Solc filter. Experience so far has indicated that these tolerances probably have to be much smaller than those required for Lyot filters. Evans (1963) found, for example, that a Solc-A filter with a tolerance of $\pm 1/40$ order on the plate thicknesses and ± 10 min on the plate orientations had a transmission curve which was very different from what one would have expected theoretically. For Lyot filters these tolerances are well within the generally accepted tolerance limits [$\pm 1/20$ order in thickness (Billings, et al., 1951) and ± 30 min (Giovanelli, et al., 1954)]. For this Solc filter they were evidently too large.

In the following, the influence resulting from small variations in the plate thicknesses and orientations on the ratio T_p/T_m will be determined (see Sec. 3.4 for the definition of T_p/T_m). This will be done with the present ray-tracing program since an analytical determination seemed to be too complicated. A third important tolerance, namely the accuracy within which the optical axis of the crystal has to lie in the element's surface, could not be treated with the present program.

3.5.2 TOLERANCES IN THE PLATE ORIENTATION

In order to study the changes in T_p/T_m , we introduced errors in the angles of the Solc-C filter plates as listed in Table 11. These errors were introduced by adding angles which were generated at random between $-\delta$ and $+\delta$ degrees, where δ represents the tolerance on the plate orientation. These small errors in the orientation were generated in the $(-\delta, +\delta)$ interval such that they have equal probability of occurring anywhere in this interval. In reality, error-distribution may be quite different from this rectangular distribution. However, as long as the actual distribution is unknown, the rectangular one seems to be as good as any.

Table 15 lists the values for T_p/T_m as computed for $\delta = 0.0, 0.5$, and 2.0 deg. They represent averages of the results of three computations, each using an independent set of random errors. All the data are also shown in Figure 11. The T_m is always defined as the total transmission in a wavelength band which has as its width the distance between the first minima as measured for the filter with $\delta = 0$, and which has a position such that T_m is maximum. Consequently, this position may deviate slightly from the position for the $\delta = 0$ deg filter. The T_p is defined as the total transmission outside this band.

Table 15. Influence of Errors in Plate Orientation and Thickness on T_p/T_m

Filter	Tolerance		T_p/T_m (%)
	Thickness (order)	Orientation (deg)	
Solc C	± 0.00	± 0.0	4.5
Solc C	± 0.00	± 0.5	5.3
Solc C	± 0.00	± 2.0	23.5
Solc C	± 0.01	± 0.0	20.1
Solc C	± 0.05	± 0.0	374.4
Solc A(5)	± 0.00	± 0.0	8.5
Solc A(5)	± 0.02	± 0.0	25.8
Solc A(15)	± 0.00	± 0.0	21.6
Solc A(15)	± 0.02	± 0.0	64.2
Solc A(45)	± 0.00	± 0.0	27.4
Solc A(45)	± 0.02	± 0.0	248.2

A tolerance of $\delta = 0.5$ deg seems to influence the performance of this type of Solc filter very little. This is rather remarkable since it represents a very large fraction of the orientations of the plates with respect to each other. In reality an orientation tolerance of ± 0.2 deg and better is attainable without much difficulty.

From Figure 11 it may also be seen that one of the computations at $\delta = 0.5$ deg actually resulted in a $T_p/T_m = 4.0$ percent, which is smaller than T_p/T_m for the $\delta = 0$ deg filter. This shows that the angles listed in Table 11 are not the optimum orientations for this filter, at least when this optimum is defined by the T_p/T_m . When we define the T_m as the transmission in a band with a width equal to the halfwidth of the main band, this particular $\delta = 0.5$ deg filter turns out to be worse than the $\delta = 0$ deg filter.

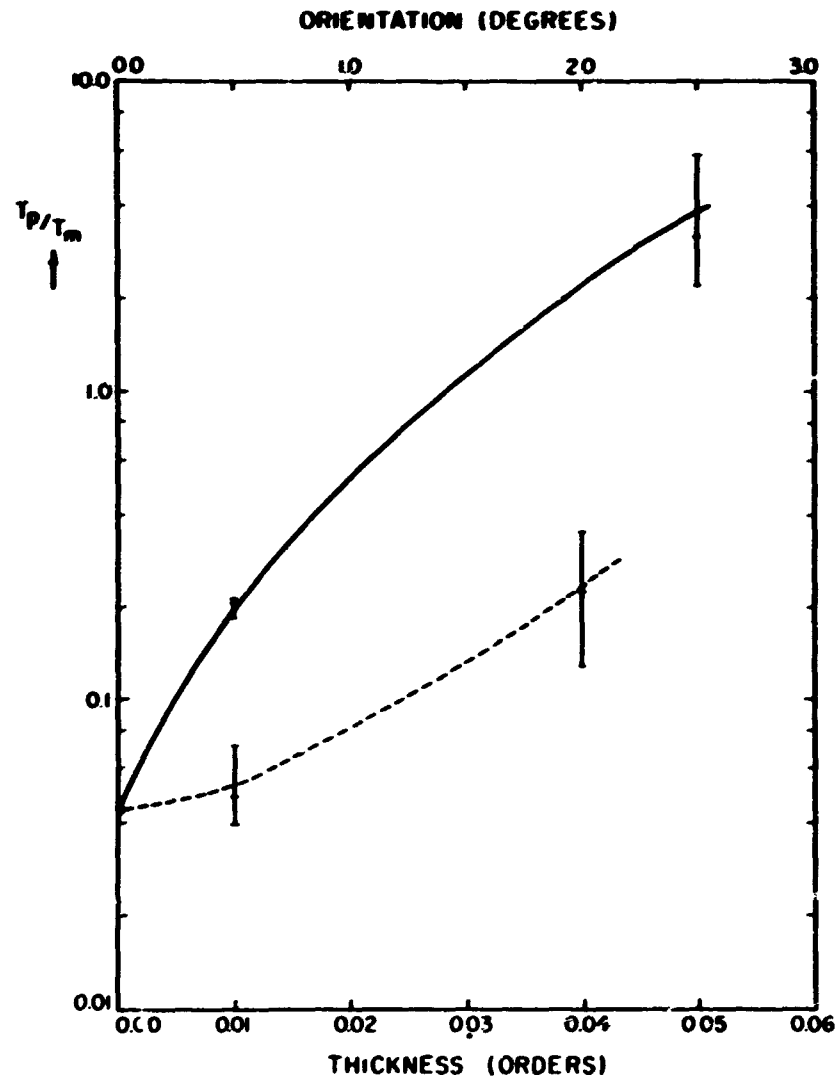


Figure 11. Ratio T_p/T_m for a Solc-C Filter with Various Tolerances for the Plate Thicknesses and Orientations. Abscissa gives maximum allowed deviation from the perfect plate in orders and degrees – solid curve for thicknesses, dashed for orientation

3.5.3 TOLERANCES IN THE PLATE THICKNESS

The same procedure is used for introducing errors in the plate thicknesses. For the Solc-C filter listed in Table 11 computations are made for tolerances $\pm \Delta$ where Δ equals 0.00, 0.01, and 0.05 orders. Table 15 lists the averages of three calculations, Figure 11 gives the individual calculations. The usual thickness tolerance for Lyot filters, $\Delta = 0.05$, now gives an increase of about 80 times over the T_p/T_m for a $\Delta = 0.0$ filter. The tolerances have to be very much smaller than those for the Lyot filter. How small they have to be depends on the requirements

one puts on the T_p/T_m . For example, if one requires T_p/T_m to be less than 1.5 times the $\Delta = 0.00$ value, one specifies a tolerance smaller than $\Delta \approx 0.002$ orders. As far as manufacturing capabilities go, this seems quite unattainable ($\Delta = 0.002$ at 5400 \AA , corresponds to thickness variations of 0.2λ and 0.01λ for quartz and calcite respectively).

Hence, it appears that the performance of a Šolc filter for on-axis rays depends very much on the art of producing birefringent plates of identical thicknesses. Having made a set of nearly identical plates, the question arises whether one can optimize the filter transmission by arranging the plates in a proper sequence. Studying the properties of a Šolc filter on the Poincaré sphere, we had the impression that errors in the thicknesses of the innermost plates would affect the filter performance more than errors on the outer plates. Calculations for the 18-plate Šolc-C filter as shown in Figure 12 confirm this. In these calculations the thickness of only one plate was changed by $1/20$ order from their perfect value, the other plates remained unchanged. The resulting T_p/T_m is actually nearly proportional to the plate number as counted from the outside of the filter, reaching 81 percent for the ninth and tenth plates at the filter core. In the construction of a Šolc filter, one can therefore gain appreciably in filter performance by placing the plates that are closest to being identical in thickness near the center of the filter.

The tolerance placed on the plate thickness will also be a function of the number of plates in the filter. In order to obtain some information about this, we computed the T_p/T_m for three Šolc-A filters with 5, 15, and 45 plates, respectively, for $\Delta = 0.00$ and $\Delta = 0.02$ orders. Table 15 lists the results that are also shown in Figure 13. The relative amount of parasitic light increases rapidly with the number of plates used in the filter when the tolerances remain the same. One has to have a much closer tolerance for filters with a large number of plates than for smaller filters. This makes productions of Šolc filters even more difficult than already indicated in the previous paragraph, since one often requires filters with more than 18 plates.

Notwithstanding these stringent requirements on the plate thicknesses, Šolc has managed to produce an 80-plate filter with reasonably low secondary transmissions (Valniček, 1960) which certainly shows the excellent technical capability of the Šolc group.

4. CONCLUSIONS

The birefringent ray-tracing program described here has turned out to be very useful for those problems connected with birefringent filters that are hard to

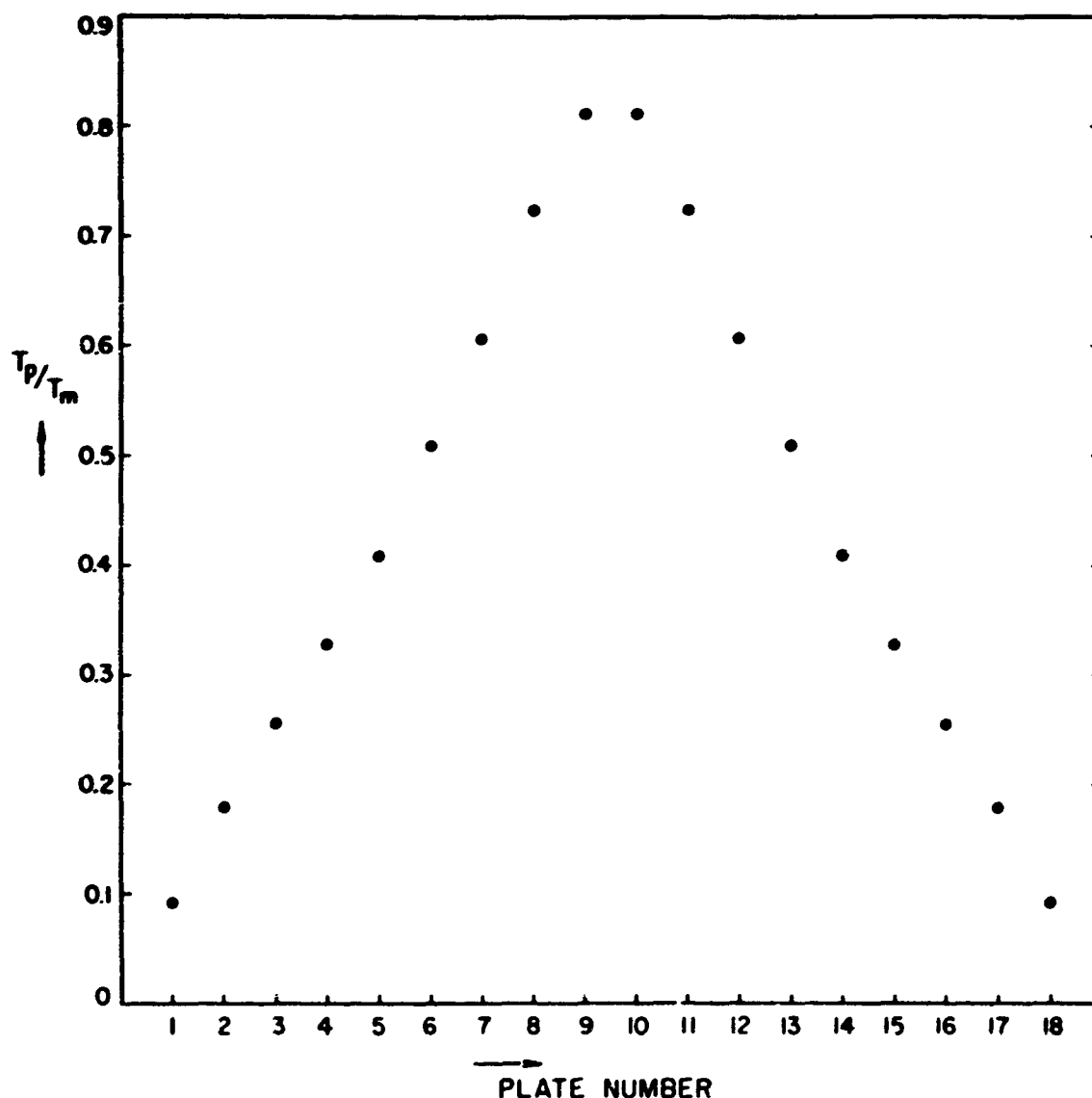


Figure 12. Ratio T_p/T_m for an 18-Plate Solc-C Filter for which Only One Plate Has a 0.05 Order Imperfection as a Function of the Plate Position

examine analytically. Machine computations of this type are still very time consuming so that filter design, like determining the best orientations for a Solc-C filter so as to give a minimum T_p/T_m , would be a major problem. The program is very suitable for determining the characteristics of a filter whose composition is given. In the future it should be worthwhile for anyone who wants to design filters to study the possibility of building an electrical circuit that is analogous to a birefringent filter. If this could be done in such a way that one could, for example, determine the "transmission" of this circuit for various voltage frequencies, one would have a very fast and powerful tool in testing various birefringent filters.

In Sec. 3 a good deal of attention was given to Solc filters. There have been many discussions in the literature about the merits of these filters with respect to the Lyot filter. The great advantage over the Lyot filter is the low number of polarizers needed. Another advantage is the lower amount of parasitic light, at least in the Solc-C type filter. The main disadvantage is the difficulty of the production of such a filter, especially when a wide-angle filter is wanted. Both the number of plates and the thickness tolerances on these plates are an order of magnitude worse than in an equivalent Lyot filter (for a normal size Solc filter of about 50 plates). Another disadvantage is that the filter's tuning can only be done by changing the filter temperature or by making each element out of two complementary wedges (Evans, 1963).

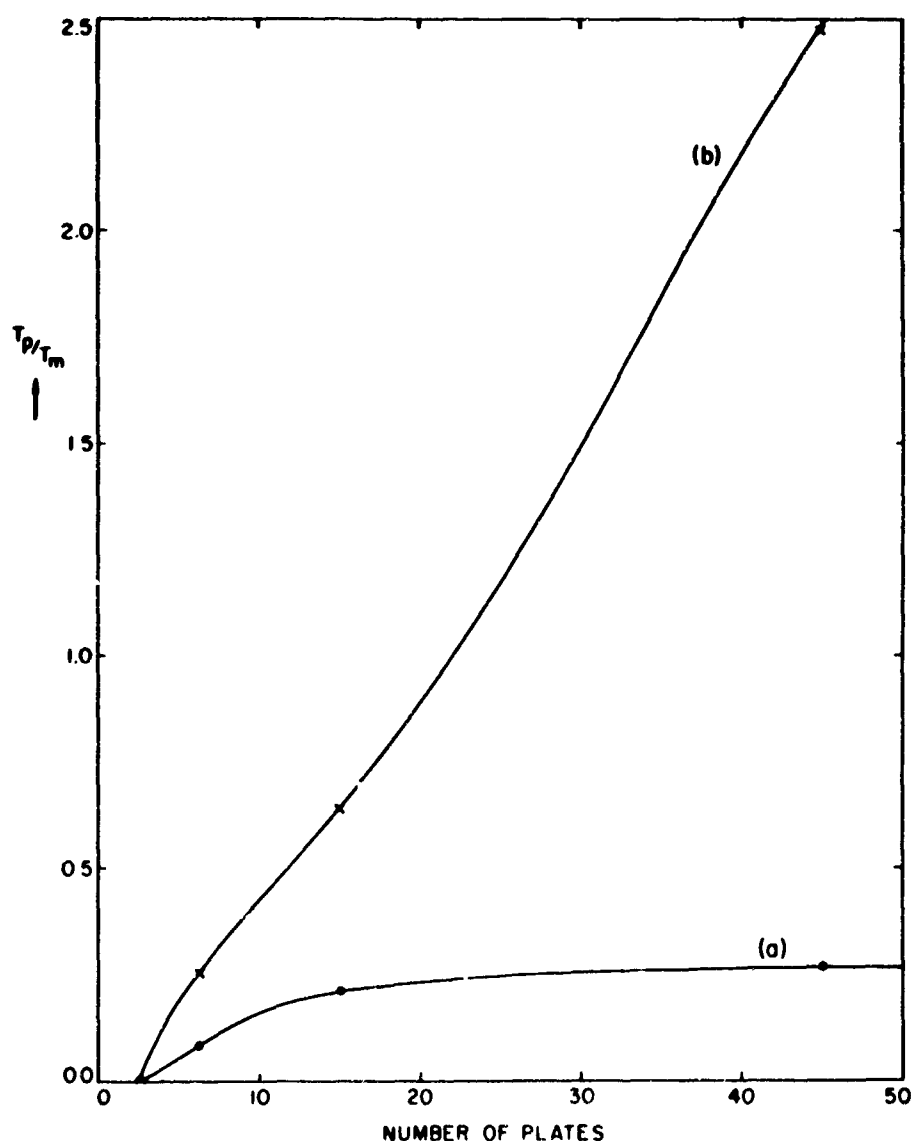


Figure 13. Ratio T_p/T_m for Solc-A Filters. Curve (a) for perfect plates, Curve (b) for filters in which plates have errors up to 0.02 orders

Acknowledgments

The authors want to express their thanks to Dr. J. W. Evans for the many useful discussions and helpful suggestions in connection with this work, and to R. Shutt for writing the computer program described in Sec. 3.2.1.2, para. (4) and the random number generator which was used in Sec. 3.5.

References

- Billings, B. H., Sage, S., and Draisin, W. (1951) A narrow passband polarization interference filter for H_{α} , Rev. Sci. Instr. 22:1009.
- Evans, J. W. (1949) The birefringent filter, J. Opt. Soc. Am. 39:229.
- Evans, J. W. (1958) Solc birefringent filter, J. Opt. Soc. Am. 48:142.
- Evans, J. W. (1963) A birefringent monochromator for isolating high orders in grating spectra, Appl. Optics 2:193.
- Giovanelli, R. G., and Jefferies, J. T. (1954) On the optical properties of components for birefringent filters, Australian J. Phys. 7:254.
- Jones, R. C. (1941) A new calculus for the treatment of optical systems, J. Opt. Soc. Am. 31:488.
- Lýot, B. (1944) Le filtre monochromatique polarisant et ses applications en physique solaire, Ann. d'Astrophysique 7:15.
- Macé de Lepinay, M. J. (1892) Sur la double refraction du quartz, Journal de Physique, 3^e série, I, 23, 1892.
- Mascart (1874), Ann. Sci. de l'Ecole Normale Supérieure 3:395.

- Shurcliff, W. A. (1962) Polarized Light, Harvard University Press, Cambridge, Mass.
- Šolc I. (1959) Chain birefringent filters, Czechosl. J. Phys. 9: 237.
- Šolc I. (1960) Chain birefringent filters, Českosl. Časopis pro Fysiku 10: 16.
- Šolc I. (1965) Chain birefringent filters, J. Opt. Soc. Am. 55: 621.
- Valnicek, B. (1960) Šolc birefringent filter composed of a large number of plates, Bull. Astr. Inst. Czechosl. 11: 162.

INSTRUMENTATION PAPERS
(Formerly: Instrumentation for Geophysics and Astrophysics)

- No. 1. A Digital Electronic Data Recording System for Pulse-Time Telemetry, *Gilbert O. Hall, Feb 1953.*
- No. 2. A Rocket-Borne Equipment for the Measurement of Infrared Radiation, *R. M. Slavin, Feb 1953.*
- No. 3. Balloon-Borne Conductivity Meter, *S. C. Coroniti, A. Nazarek, C. S. Stergis, D. E. Kotas, D. W. Seymour and J. V. Verme, Dec 1954.*
- No. 4. Magnetic Compensation of Aircraft, *J. McClay and B. Schuman, Aug 1955.*
- No. 5. Lovotron-A Low Voltage Triggered Gap Switch, *E. H. Cullington, W. G. Chace and R. L. Morgan, Sep 1955.*
- No. 6. Balloon-Borne Air Sampling Device, *Charles W. Chagnon, Apr 1957.*
- No. 7. Instrumentation for Studies of the Exploding Wire Phenomenon, *W. G. Chace and E. H. Cullington, Aug 1957.*
- No. 8. Device for Lowering Loads from High-Altitude Balloons, *W. C. Wagner and F. X. Doherty, Jul 1958.*
- No. 9. Equipment and Techniques for In-Flight Deployment of Long Train Instrumentation Packages from High Altitude Balloons, *Arlo E. Gilpatrick and Romain C. Fruge, Sep 1958.*
- No. 10. Study of a Phosphor Light Pulsar, *Michael R. Zatzick, Sep 1960.*
- No. 11. Study of a Pulsed Logarithmic Photometer, *Michael R. Zatzick, Sep 1960.*
- No. 12. Theoretical Analysis of the PAR-Scope: An Oscilloscope Display for Weather Radars, *Edwin Kessler, III, Jul 1959.*
- No. 13. Evaluation of Visual Distance Computer, CP-384(XD-1), *P. I. Hershberg, Apr 1960.*
- No. 14. Hypsometer for Constant Level Balloon, *W. C. Wagner, Jun 1960.*
- No. 15. Magnetic Photomultiplier with Large Cathode for Extreme Ultraviolet, *L. A. Hall and H. E. Hinteregger, Dec 1960.*
- No. 16. AIDE - Altitude Integrating Device, Electronic, *P. I. Hershberg, J. R. Griffin and R. H. Guenther, Dec 1960.*
- No. 17. Switching Devices for Very High Currents, *E. H. Cullington and W. G. Chace, April 1961.*
- No. 18. Cedar Hill Meteorological Research Facility, *D. W. Stevens, Jun 1961.*
- No. 19. Evaluation of Control Monitor AN/GGA 11 Prototype, *R. S. Menchel, Aug 1961.*
- No. 20. A Microwave Refractometer with Fast Response and Absolute Digital Recording, *R. H. Shaw and R. M. Cunningham, Mar 1962.*
- No. 21. Superpressure Balloon for Constant Level Flight, *L. Gruss, Jul 1962.*
- No. 22. Measurement Range Required of Meteorological Equipment, *A. Court and H. Salmela, Aug 1962.*
- No. 23. Proportional Counter Spectrometer for Solar X-Rays Between 1 and 10 Angstroms, *L. Heroux, J. E. Manson, and R. Smith, Dec 1962.*
- No. 24. A Simplified Sonic Anemometer for Measuring the Vertical Component of Wind Velocity, *J. Chandran Kaimal, Jan 63.*
- No. 25. Evaluation of Modification to Antenna of Rawin Set AN/GMD-2, *Konstantin Pocs, Jan 63.*
- No. 26. Evolution of the Design of the Anna I Satellite Optical Beacon, *T. Wirtanen, Feb 63.*
- No. 27. Seismic Model Impactor, *K. C. Thomson and J. A. Hill, Aug 63.*
- No. 28. Error Analysis of the Modified Humidity-Temperature Measuring Set AN/TMQ-11, *R. W. Lenhard, Jr., Major, USAF, and B. D. Weiss, Aug 63.*
- No. 29. Evaluation of a Varactor Diode Parametric Amplifier for Rawin Set AN/GMD-2, *Konstantin Pocs, Sep 1963.*
- No. 30. The Hydromagnetic Wave Tube, *R. E. Murphy and M. H. Bruce, Sep 1963.*
- No. 31. A Time-of-Flight Mass Spectrometer Adapted for Studying Charge Transfer, Ion Dissociation, and Photoionization, *W. Hunt, Jr., et al., Sep 1963.*
- No. 32. Moire Fringe Measuring System for Far Infrared Interferometric Spectrometer, *E. V. Loewenstein, Sep 1963.*
- No. 33. Opposed Anvil Basic Design Considerations, *R. E. Riecker, 1/Lt USAF, Dec 1963.*
- No. 34. New Shear Apparatus for Temperatures of 1000°C and Pressures of 50 kb, *R. E. Riecker, 1/Lt USAF, K. E. Seifert, 1/Lt USAF, Nov 1963.*
- No. 35. Accuracy of Meteorological Data Obtained by Tracking the ROBIN With MPS-19 Radar, *Robert W. Lenhard, Jr., Major, USAF, Margaret P. Doody, Dec 1963.*
- No. 36. An Application of Induction Heating to Rock Deformation Apparatus, *R. E. Riecker, 1/Lt, USAF, Mar 1964.*
- No. 37. A Monopole Phased-Array Feed for Spherical Reflectors, *W. G. Havroides, L. S. Dorr, April 1964.*
- No. 38. Equipment and Techniques for Low Temperature Electron Irradiations, *L. F. Lowe, C. Jimenez, and E. A. Burke, April 1964 (REPRINT).*
- No. 39. Lunar Thermal Emission Measurements and Related Antenna Considerations, *John P. Castelli, April 1964 (REPRINT).*
- No. 40. Continuous Zone-Refining Apparatus, *John K. Kennedy, April 1964 (REPRINT).*

INSTRUMENTATION PAPERS (Continued)

- No. 41. Improved Closed-System Evaporation Crystallizer, *John L. Sampson and Mary A. DiPietro, May 1964 (REPRINT).*
- No. 42. Calibration of a Flyable Mass Spectrometer for N and O Atom Sensitivity, *R.S. Narcisi, H.J. Schiff, J.E. Morgan and H.A. Cohen, June 1964 (REPRINT).*
- No. 43. A Preliminary Evaluation of the Cricketsonde Rocket System, *Konstantins Pocs, June 1964.*
- No. 44. New Shear Apparatus for Temperatures of 1000°C and Pressures of 50 Kilobars, *R.E. Riecker, August 1964 (REPRINT).*
- No. 45. Reflection Correction for Thermal Neutron Spectra Derived from Transmission Data, *E.A. Burke and L.F. Lowe, August 1964 (REPRINT).*
- No. 46. A Prototype Lunar Transponder, *Mahlon S. Hunt, August 1964 (REPRINT).*
- No. 47. Automatic Plotting of Spin-Wave Instability Threshold Data, *Tom G. Purnhagen, Capt, USAF, August 1964 (REPRINT).*
- No. 48. Logical Techniques for Clottal Source Measurements, *John L. Ramsey, 1/Lt, USAF, August 1964.*
- No. 49. An Ultrastable Microwave Radiometer, *William B. Goggins, Jr., Capt, USAF, September 1964.*
- No. 50. Impurities in a Vacuum, *Jerome H. Bloom, Charlotte E. Ludington, and Robert L. Phipps, May 1964.*
- No. 51. Digital Readout of Oscilloscope Sweep Delay Times, *K.E. McGee and W.W. Hunt, Jr., October 1964 (REPRINT).*
- No. 52. High Pressure Thrust Bearings: An Application, *R.E. Riecker and D.L. Pendleton, November 1964.*
- No. 53. A Method for Electrocutting Single Crystals of Metals and Electropolishing the Exposed Crystalline Face, *Bernard Rubin and John J. O'Connor, December 1964.*
- No. 54. Comparison of Bivane and Sonic Techniques for Measuring the Vertical Wind Component, *J.C. Kaimal, H.E. Cramer, F.A. Record, J.E. Tillman, J.A. Businger, and M. Miyake, December 1964 (REPRINT).*
- No. 55. Experiences with the Impedance Probe on Satellites, *O.C. Haycock, K.D. Baker and J.C. Ulwick, January 1965 (REPRINT).*
- No. 56. Silicon Current Amplifier for Microampere Current Levels, *B. Buchanan, S. Roosild, and R. Dolan, February 1965 (REPRINT).*
- No. 57. A Multi-Level Radar Storm Contour Mapper, *William E. Lamkin and David Atlas, April 1965.*
- No. 58. Nanosecond Pulses of Very Low Impedance, *Heinz J. Fischer, April 1965.*
- No. 59. An Operational Amplifier Circuit for Characterization of Negative-Conductance Devices, *Virgil E. Vickers, April 1965 (REPRINT).*
- No. 60. Multiband Spectral System for Reconnaissance, *Carlton E. Molineux, April 1965 (REPRINT).*
- No. 61. Operating Characteristics of a Commercial Resistance-Strip Magnetic Electron Multiplier, *W.W. Hunt, Jr., K.E. McGee, and M.J. Kennedy, May 1965 (REPRINT).*
- No. 62. Frequency Stability in Dielectric Resonators, *M.R. Stiglitz and J.C. Sethares, May 1965 (REPRINT).*
- No. 63. ANNA Satellite Yields Photogrammetric Parameters, *Owen W. Williams, June 1965 (REPRINT).*
- No. 64. Heat Transfer Considerations in the Temperature Control of Instrumentation Packages at High Altitudes, *Arnold Piacentini, Kenneth H. Linänselser, 1/Lt, USAF, and Darrel E. Dube, 1/Lt, USAF, June 1965.*
- No. 65. Vacuum Ultraviolet Light Sources: New Excitation Unit for the Rare Gas Continua, *R.E. Huffman, J.C. Larrabee, and Derek Chambers, June 1965.*
- No. 66. The Compensation of Two-Beam Interferometers, *W.H. Steel, June 1965.*
- No. 67. A Laser Fog Disdrometer, *Bernard A. Silverman, Brian J. Thompson, and John H. Ward, June 1965 (REPRINT).*
- No. 68. Radiochemical Procedures for Selected Radionuclides in Environmental Samples, *Joseph Pecci, Peter J. Drevinsky, Edward Couble, Noreen A. Dimond, Marvin I. Kalkstein, and Anahid Thomasian, June 1965.*
- No. 69. Evaluation of the T-755/GMQ-20 Wind Speed and Direction Transmitter, *Russell M. Peirce, Jr., June 1965.*
- No. 70. A Laser for an Earth-Based Satellite Illuminator, *Robert L. Iliff, June 1965.*
- No. 71. A Unique Scintillation Rate Counter for Ionospheric Studies, *Frederick F. Slack and John P. Mullen, June 1965.*
- No. 72. Differential Thermal Analysis (DTA) of Oxide Systems in Air to 1620°C at Atmospheric Pressure, *Cortland O. Dugger, June 1965.*
- No. 73. Automatic Camera System for Solar Corona Photography, *D.J. Davis, Jr., W.R. McCann, V.A. Remillard, P. Beaudouin, and A. Thomas, July 1965 (REPRINT).*
- No. 74. A Direct Calibration of a Birefringent Photometer, *G.J. Hernandez and E.L. Layman, August 1965 (REPRINT).*
- No. 75. A Ray-Tracing Program for Birefringent Filters, *J.M. Beckers, and R.B. Dunn, August 1965.*

Unclassified
Security Classification

DOCUMENT CONTROL DATA - R&D		
(Security classification of title, body of abstract and indexing annotation must be entered when the overall report is classified)		
1. ORIGINATING ACTIVITY (Corporate author) Hq AFCRL, OAF. (CRF) United States Air Force Bedford, Massachusetts		2a. REPORT SECURITY CLASSIFICATION Unclassified 2b. GROUP -
3. REPORT TITLE A Ray-Tracing Program for Birefringent Filters		
4. DESCRIPTIVE NOTES (Type of report and inclusive dates) Scientific Report. State of the art.		
5. AUTHOR(S) (Last name, first name, initial) BECKERS, J. M. and DUNN, Richard B.		
6. REPORT DATE August 1965	7a. TOTAL NO. OF PAGES 56	7b. NO. OF REFS 14
8a. CONTRACT OR GRANT NO. - A. PROJECT AND TASK NO. 7649-06 C. DOD ELEMENT 62405394 d. DOD SUBELEMENT 681000		9a. ORIGINATOR'S REPORT NUMBER(S) AFCRL-65-605 9b. OTHER REPORT NO(S) (Any other numbers that may be assigned this report) AFCRL-65-605
10. AVAILABILITY/LIMITATION NOTICES Qualified requestors may obtain copies of this report from DDC. Other persons or organizations should apply to the Clearinghouse for Federal Scientific and Technical Information (CFSTI), Sills, Building, 5285 Port Royal Road, Springfield, Virginia 22151.		
11. SUPPLEMENTARY NOTES	12. SPONSORING MILITARY ACTIVITY Hq AFCRL, OAR (CRF) United States Air Force Bedford, Massachusetts	
13. ABSTRACT <p>A computer program for determining the transmission of birefringent filters is described. This program is used for the following investigations.</p> <p>a) The feasibility of the construction of a birefringent filter that will work simultaneously for wavelengths of 3933.3, 6562.8, and 10830.3 Angstroms. These three wavelengths are of particular importance for solar studies.</p> <p>b) The off-axis characteristics of Solc filters.</p> <p>c) The tolerances required for the elements of a Solc filter.</p> <p>d) The influence of imperfect polarizers on the transmission characteristics of Lyot filters.</p>		

DD FORM 1473
1 JAN 64

Unclassified
Security Classification

Unclassified
Security Classification

14. KEY WORDS	LINK A		LINK B		LINK C	
	ROLE	WT	ROLE	WT	ROLE	WT
Solar studies Birefringent filter transmission						

INSTRUCTIONS

1. ORIGINATING ACTIVITY: Enter the name and address of the contractor, subcontractor, grantee, Department of Defense activity or other organization (*corporate author*) issuing the report.

2a. REPORT SECURITY CLASSIFICATION: Enter the overall security classification of the report. Indicate whether "Restricted Data" is included. Marking is to be in accordance with appropriate security regulations.

2b. GROUP: Automatic downgrading is specified in DoD Directive 5200.10 and Armed Forces Industrial Manual. Enter the group number. Also, when applicable, show that optional markings have been used for Group 3 and Group 4 as authorized.

3. REPORT TITLE: Enter the complete report title in all capital letters. Titles in all cases should be unclassified. If a meaningful title cannot be selected without classification, show title classification in all capitals in parenthesis immediately following the title.

4. DESCRIPTIVE NOTES: If appropriate, enter the type of report, e.g., interim, progress, summary, annual, or final. Give the inclusive dates when a specific reporting period is covered.

5. AUTHOR(S): Enter the name(s) of author(s) as shown on or in the report. Enter last name, first name, middle initial. If military, show rank and branch of service. The name of the principal author is an absolute minimum requirement.

6. REPORT DATE: Enter the date of the report as day, month, year, or month, year. If more than one date appears on the report, use date of publication.

7a. TOTAL NUMBER OF PAGES: The total page count should follow normal pagination procedures, i.e., enter the number of pages containing information.

7b. NUMBER OF REFERENCES: Enter the total number of references cited in the report.

8a. CONTRACT OR GRANT NUMBER: If appropriate, enter the applicable number of the contract or grant under which the report was written.

8b, 8c, & 8d. PROJECT NUMBER: Enter the appropriate military department identification, such as project number, subproject number, system numbers, task number, etc.

9a. ORIGINATOR'S REPORT NUMBER(S): Enter the official report number by which the document will be identified and controlled by the originating activity. This number must be unique to this report.

9b. OTHER REPORT NUMBER(S): If the report has been assigned any other report numbers (*either by the originator or by the sponsor*), also enter this number(s).

10. AVAILABILITY/LIMITATION NOTICES: Enter any limitations on further dissemination of the report, other than those imposed by security classification, using standard statements such as:

- (1) "Qualified requesters may obtain copies of this report from DDC."
- (2) "Foreign announcement and dissemination of this report by DDC is not authorized."
- (3) "U. S. Government agencies may obtain copies of this report directly from DDC. Other qualified DDC users shall request through _____."
- (4) "U. S. military agencies may obtain copies of this report directly from DDC. Other qualified users shall request through _____."
- (5) "All distribution of this report is controlled. Qualified DDC users shall request through _____."

If the report has been furnished to the Office of Technical Services, Department of Commerce, for sale to the public, indicate this fact and enter the price, if known.

11. SUPPLEMENTARY NOTES: Use for additional explanatory notes.

12. SPONSORING MILITARY ACTIVITY: Enter the name of the departmental project office or laboratory sponsoring (*paying for*) the research and development. Include address.

13. ABSTRACT: Enter an abstract giving a brief and factual summary of the document indicative of the report, even though it may also appear elsewhere in the body of the technical report. If additional space is required, a continuation sheet shall be attached.

It is highly desirable that the abstract of classified reports be unclassified. Each paragraph of the abstract shall end with an indication of the military security classification of the information in the paragraph, represented as (TS), (S), (C), or (U).

There is no limitation on the length of the abstract. However, the suggested length is from 150 to 225 words.

14. KEY WORDS: Key words are technically meaningful terms or short phrases that characterize a report and may be used as index entries for cataloging the report. Key words must be selected so that no security classification is required. Identifiers, such as equipment model designation, trade name, military project code name, geographic location, may be used as key words but will be followed by an indication of technical context. The assignment of links, rules, and weights is optional.

Unclassified
Security Classification